AD-A067 395 NAVAL UNDERSEA RESEARCH AND DEVELOPMENT CENTER SAN D--ETC F/G 17/1
EVALUATION OF NEOTRON SONAR AMPLIFIER MODULE,(U)
APR 71 J M CHRISTIAN

UNCLASSIFIED NUC-TN-517 NL

| OF |
AD
A067395

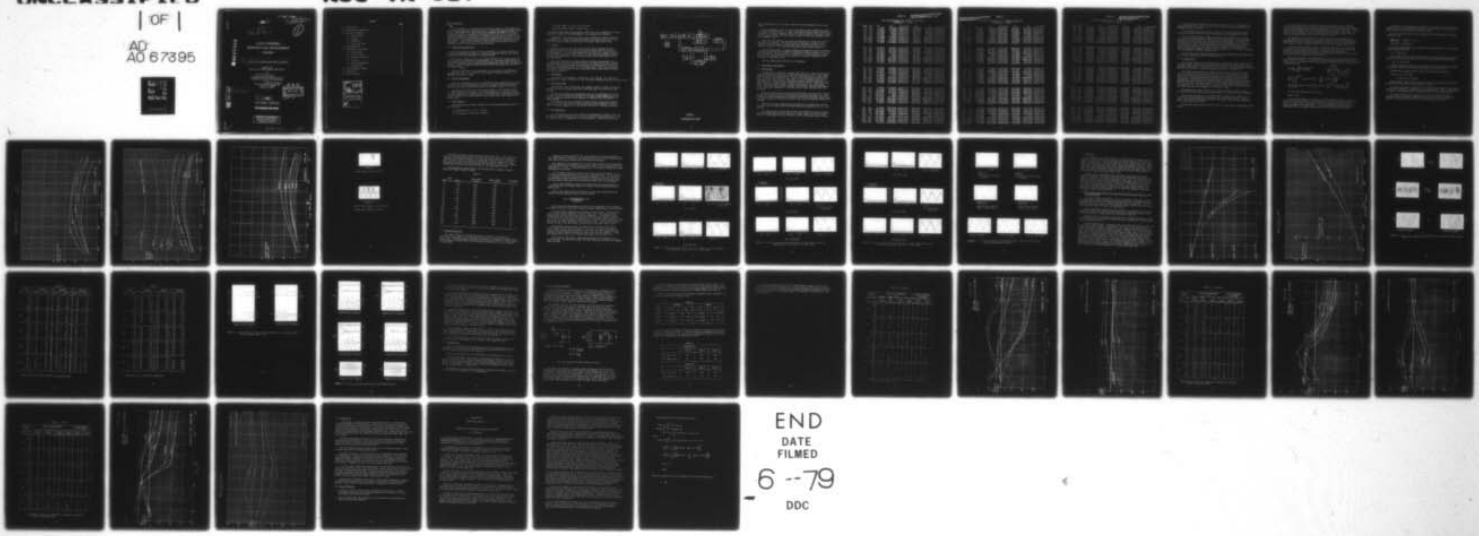

END
DATE
FILMED
6 -79
DDC

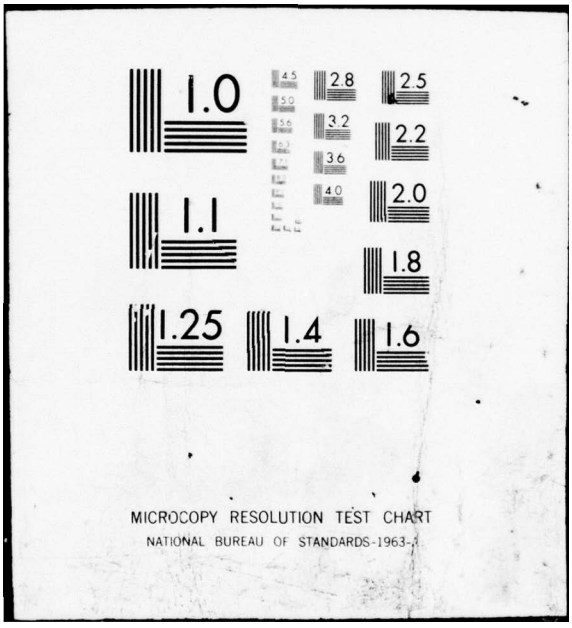
1.0
1.1
1.25
1.4
1.6
1.8
2.0
2.2
2.5
2.8
3.2
3.6
4.0
4.5
5.0
5.6
6.3
MICROCOPY RESOLUTION TEST CHART
NATIONAL BUREAU OF STANDARDS-1963-A

NAVAL UNDERSEA RESEARCH AND DEVELOPMENT CENTER

(6) EVALUATION OF NEOTRON SONAR AMPLIFIER MODULE,

Prepared for
Naval Ship Systems Command (NSHP-00V1D)

By

(10) J. M. Christian
Transducer and Array Systems Division
Sensor and Fire Control Department

(17) Subproject No. SF 11 121 301
Element No. 62503N
Task No. 14062

(11) April 1971

San Diego, California

~~FOR OFFICIAL USE ONLY~~

CONTENTS

1.0 Introduction

This experiment is an evaluation of the Neotron Amplifier Module, developed by the Amperex Electronic Corporation under the Naval Electronics Systems Command contract N00039-69-C-2542. The manufacturers January 15, 1970 report "Final Development Report for Feasibility Investigation of A Neotron in A Conduction - Cooled Sonar Amplifier Module" gives a complete description and pictures of the amplifier module plus development procedures followed and manufacturer's evaluation results. Five identical complete amplifier modules were furnished for our evaluation. A module test fixture with water-cooled cooling plate and interconnecting cables to the module was also furnished.

2.0 Motivation and Objectives

There were two main reasons for this experiment. The first concerns the request from NAVSHIPS Code 00V1D to evaluate the amplifier modules and compare our results with those published by the manufacturer.

The second concerns a part of the "Sonar Amplifier Task" assigned Code 601 which consists of evaluation of representative or interesting sonar amplifiers via specific voltage, current and phase measurements and then using this empirical data in a computer program determine Norton and Thevenin equivalent circuits for the amplifier.

The major objective of this experiment is to evaluate the performance of the amplifier as is. Not to correct or necessarily indicate reasons for any anomalies that might be found.

3.0 General Information

Since our measurements are to be compared with those published by the manufacturer in his final development report, our amplifier operating conditions, range of loads and frequencies are basically the same as those in the report.

The amplifier system in our test setup consists of the following items: (1) signal generator, (2) keyer or tone pulse generator, (3) amplifier module, (4) four external power supplies, and (5) electrical load. The amplifier module itself is made up of a driver amplifier and a final power output section (the Neotron tube).

3.1 Power Supplies

The external power supplies required for the Neotron amplifier consist of the following:

(1) Filament supply (5 v.dc. @ 7 amps)

(2) Bias supply (- 300 v.dc. @ 100 ma.)

(3) Driver supply (+ 150 v.dc. @ 150 ma.)

(4) Neotron plate supply (+ 5400 v.dc.)

The plate voltage supply rating needed is 5400 v.dc. with a capability of supplying current pulses of four peak amperes at the frequency of operation.

Regulation of our supply was poor so that unloaded, the voltage climbed to about 6000 v.dc. However no power measurements were made during a pulse until the plate supply voltage settled down to the proper steady state value.

3.2 Cooling

Module cooling for the bench tests was provided by flowing tap water through the heat sink at the rear of the module testing fixture furnished by the manufacturer. The tap water temperature ran about 25°C. Normal operation at full power at a 5 sec. on and 45 sec. off duty cycle would barely increase the heat sink temperature, but an increase in duty cycle would quickly raise the temperature.

Where only one module is being cooled no problem is encountered, but if several modules were to be cooled in series by the same flow of water, heating could be a real problem and the limit imposed by the manufacturer of 50°C for the heat sink temperature might be hard to stay below. Tests and calculations would have to be performed in order to determine exactly what would be needed for a given condition.

3.3 Frequencies

The amplifier was designed to operate at 5 kHz $\pm$ 500 Hz. Our tests were performed at 4.5 kHz, 5.0 kHz and 5.5 kHz, the same frequencies used by the manufacturer.

3.4 Electrical Loads

The amplifier output transformer has impedance taps at 10 ohms, 20 ohms and 50 ohms. We chose to operate with the 50 ohm tap, again the same as the manufacturer.

Our electrical loads for the amplifier were for the magnitudes of 15 ohms, 50 ohms, 80 ohms, 120 ohms and 150 ohms, with relative phase angles between the output voltage and current of zero degrees, $\pm$ 30 degrees and $\pm$ 60 degrees for each magnitude.

The manufacturers tests encompassed those values by using load conditions varying in 15 ohm steps from 15 ohms to 150 ohms at phase angles that varied from - 60 degrees capacitive to + 60 degrees inductive in 15-degree increments.

4.0 Instrumentation

Our instrumentation set up to perform the measurements is shown in Fig. (1). The keyer or pulse generator used is the one furnished by the manufacturer. Set for 10% duty cycle, 5 seconds on or 5 mili-seconds on. However for some later

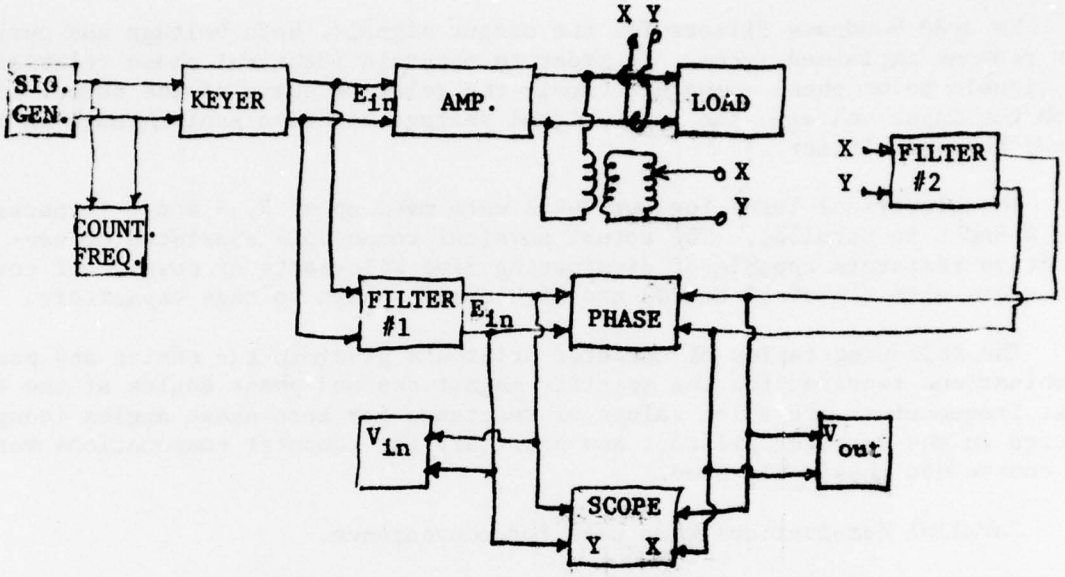

FIGURE 1

INSTRUMENTATION SETUP

delay measurements we used a phase coherent tone burst generator as the pulse source.

We used bandpass filters for the output signals, both voltage and current, for reasons explained later. In order to maintain identical phase relationships of signals to be phase compared, namely the relative phase of the output signals with the input voltage, the input signal voltage was also sent through an identical bandpass filter.

The electrical loads for our tests were made up of R, R and C in parallel and R and L in parallel. The actual physical components consisted of non-reactive resistors capable of dissipating five kilo-watts of power, air core inductors with Q's of 50 to 200 and high quality high voltage capacitors.

The following tables of computer printouts give both the series and parallel combinations required for the specific magnitudes and phase angles at the three test frequencies. Parallel values of reactance for zero phase angles though listed in the computer printout and necessary for computer computations were of course not physically used.

Parallel combinations were used for convenience.

5.0 Measurements and Results

5.1 *Output Power*

The amplifier is designed to deliver 2500 watts into a 50-ohm non-reactive load (on the 50-ohm output tap) at 5000 Hz when properly cooled. Input signal level required to the module driver for full power out under the above conditions is 100 mv. rms to 500 mv. rms. That is, the driver gain can be set for any signal level between 100 mv. and 500 mv. and will drive the amplifier to full power out. In our setup we adjusted the driver gain for 2500 watts output into a 50-ohm non-reactive load at 5000 Hz using 500 mv. rms. input signal level. The input level and gain settings then remained fixed for measurements at the three test frequencies. A 10% duty cycle, 5 sec. on and 45 sec. off, was used.

Using the instrumentation set up described before, the input drive voltage was set to the proper level and frequency and constantly monitored, the output voltage and current magnitudes were measured and the relative phase angle between the input voltage as a reference and each of the output voltage and current was measured.

These were the basic measurements performed for the power output calculations and for the linear amplifier Thevenin and Norton equivalent circuit calculations.

The output signals, voltage and current, were filtered in order to measure only the fundamental frequency component of these signals, and as was stated before the input signal was also filtered in order to maintain phase relevance.

TABLE IA

LOAD CALCULATIONS FOR NEUTRON AMPLIFIER
FREQUENCY = 4500.

ZMAG	ANG	RS	XS	LS OR CS	RP	XP	LP OR CP
15.	60.	7.5000	12.9904	.4594D-003	30.0000	17.3205	.6126D-003
15.	45.	10.6066	10.6066	.3751D-003	21.2132	21.2132	.7503D-003
15.	30.	12.9904	7.5000	.2653D-003	17.3205	30.0000	.1061D-002
15.	15.	14.4889	3.8823	.1373D-003	15.5291	57.9555	.2050D-002
15.	0.	15.0000	.0000	.0000D 000	15.0000	1.0000	.3537D-006
15.	-15.	14.4889	-3.8823	.9110D-005	15.5291	-57.9555	.6103D-006
15.	-30.	12.9904	-7.5000	.4716D-005	17.3205	-30.0000	.1179D-005
15.	-45.	10.6066	-10.6066	.3335D-005	21.2132	-21.2132	.1667D-005
15.	-60.	7.5000	-12.9904	.2723D-005	30.0000	-17.3205	.2042D-005
50.	60.	25.0000	43.3013	.1531D-002	100.0000	57.7350	.2042D-002
50.	45.	35.3553	35.3553	.1250D-002	70.7107	70.7107	.2501D-002
50.	30.	43.3013	25.0000	.8842D-003	57.7350	100.0000	.3537D-002
50.	15.	48.2963	12.9410	.4577D-003	51.7638	193.1852	.6833D-002
50.	0.	50.0000	.0000	.0000D 000	50.0000	1.0000	.3537D-006
50.	-15.	48.2963	-12.9410	.2733D-005	51.7638	-193.1852	.1831D-006
50.	-30.	43.3013	-25.0000	.1415D-005	57.7350	-100.0000	.3537D-006
50.	-45.	35.3553	-35.3553	.1000D-005	70.7107	-70.7107	.5002D-006
50.	-60.	25.0000	-43.3013	.8168D-006	100.0000	-57.7350	.6126D-006
80.	60.	40.0000	69.2820	.2450D-002	160.0000	92.3760	.3267D-002
80.	45.	56.5685	56.5685	.2001D-002	113.1371	113.1371	.4001D-002
80.	30.	69.2820	40.0000	.1415D-002	92.3760	160.0000	.5659D-002
80.	15.	77.2741	20.7055	.7323D-003	82.8221	309.0963	.1093D-001
80.	0.	80.0000	.0000	.0000D 000	80.0000	1.0000	.3537D-006
80.	-15.	77.2741	-20.7055	.1708D-005	82.8221	-309.0963	.1144D-006
80.	-30.	69.2820	-40.0000	.8842D-006	92.3760	-160.0000	.2210D-006
80.	-45.	56.5685	-56.5685	.6252D-006	113.1371	-113.1371	.3126D-006
80.	-60.	40.0000	-69.2820	.5105D-006	160.0000	-92.3760	.3829D-006
120.	60.	60.0000	103.9230	.3676D-002	240.0000	138.5641	.4901D-002
120.	45.	84.8528	84.8528	.3001D-002	169.7056	169.7056	.6002D-002
120.	30.	103.9230	60.0000	.2122D-002	138.5641	240.0000	.8488D-002
120.	15.	115.9111	31.0583	.1098D-002	124.2331	463.6444	.1640D-001
120.	0.	120.0000	.0000	.0000D 000	120.0000	1.0000	.3537D-006
120.	-15.	115.9111	-31.0583	.1139D-005	124.2331	-463.6444	.7628D-007
120.	-30.	103.9230	-60.0000	.5895D-006	138.5641	-240.0000	.1471D-006
120.	-45.	84.8528	-84.8528	.4168D-006	169.7056	-169.7056	.2084D-006
120.	-60.	60.0000	-103.9230	.3403D-006	240.0000	-138.5641	.2552D-006
150.	60.	75.0000	129.9038	.4594D-002	300.0000	173.2051	.6126D-002
150.	45.	106.0660	106.0660	.3751D-002	212.1320	212.1320	.7503D-002
150.	30.	129.9038	75.0000	.2653D-002	173.2051	300.0000	.1061D-001
150.	15.	144.8889	38.8229	.1373D-002	155.2914	579.5555	.2050D-001
150.	0.	150.0000	.0000	.0000D 000	150.0000	1.0000	.3537D-006
150.	-15.	144.8889	-38.8229	.9110D-006	155.2914	-579.5555	.6103D-007
150.	-30.	129.9038	-75.0000	.4716D-006	173.2051	-300.0000	.1179D-006
150.	-45.	106.0660	-106.0660	.3335D-006	212.1320	-212.1320	.1667D-006
150.	-60.	75.0000	-129.9038	.2723D-006	300.0000	-173.2051	.2042D-006

TABLE IB

LOAD CALCULATIONS FOR NEUTRON AMPLIFIER
FREQUENCY = 5000.

[illegible]	[illegible]	XS	YS	LS OR CS	RP	XP	LP OR CP
15.	60.	7.5000	12.9904	.41350-003	30.0000	17.3205	.55130-003
15.	45.	10.6066	10.6066	.33760-003	21.2132	21.2132	.67520-003
15.	30.	12.9904	7.5000	.23870-003	17.3205	30.0000	.95490-003
15.	15.	14.4889	3.8823	.12360-003	15.5291	57.9555	.18450-002
15.	0.	15.0000	.0000	.00000 000	15.0000	1.0000	.31830 046
15.	-15.	14.4889	-3.8823	.81990-005	15.5291	-57.9555	.54920-006
15.	-30.	12.9904	-7.5000	.42440-005	17.3205	-30.0000	.10610-005
15.	-45.	10.6066	-10.6066	.30010-005	21.2132	-21.2132	.15010-005
15.	-60.	7.5000	-12.9904	.24500-005	30.0000	-17.3205	.18380-005
50.	60.	25.0000	43.3013	.13780-002	100.0000	57.7350	.18380-002
50.	45.	35.3553	35.3553	.11250-002	70.7107	70.7107	.22510-002
50.	30.	43.3013	25.0000	.79580-003	57.7350	100.0000	.31830-002
50.	15.	48.2963	12.9410	.41190-003	51.7638	193.1852	.61480-002
50.	0.	50.0000	.0000	.00000 000	50.0000	1.0000	.31830 046
50.	-15.	48.2963	-12.9410	.24600-005	51.7638	-193.1852	.16480-006
50.	-30.	43.3013	-25.0000	.12730-005	57.7350	-100.0000	.31830-006
50.	-45.	35.3553	-35.3553	.90030-006	70.7107	-70.7107	.45020-006
50.	-60.	25.0000	-43.3013	.73510-006	100.0000	-57.7350	.55130-006
80.	60.	40.0000	69.2820	.22050-002	160.0000	92.3760	.29400-002
80.	45.	56.5685	56.5685	.18010-002	113.1371	113.1371	.36010-002
80.	30.	69.2820	40.0000	.12730-002	92.3760	160.0000	.50930-002
80.	15.	77.2741	20.7055	.65910-003	82.8221	309.0963	.98390-002
80.	0.	80.0000	.0000	.00000 000	80.0000	1.0000	.31830 046
80.	-15.	77.2741	-20.7055	.15370-005	82.8221	-309.0963	.10300-006
80.	-30.	69.2820	-40.0000	.79580-006	92.3760	-160.0000	.19890-006
80.	-45.	56.5685	-56.5685	.56270-006	113.1371	-113.1371	.28130-006
80.	-60.	40.0000	-69.2820	.45940-006	160.0000	-92.3760	.34460-006
120.	60.	60.0000	103.9230	.33080-002	240.0000	138.5641	.44110-002
120.	45.	84.8528	84.8528	.27010-002	169.7056	169.7056	.54020-002
120.	30.	103.9230	60.0000	.19100-002	138.5641	240.0000	.76390-002
120.	15.	115.9111	31.0583	.98860-003	124.2331	463.6444	.14760-001
120.	0.	120.0000	.0000	.00000 000	120.0000	1.0000	.31830 046
120.	-15.	115.9111	-31.0583	.10250-005	124.2331	-463.6444	.68650-007
120.	-30.	103.9230	-60.0000	.53050-006	138.5641	-240.0000	.13260-006
120.	-45.	84.8528	-84.8528	.37510-006	169.7056	-169.7056	.18760-006
120.	-60.	60.0000	-103.9230	.30630-006	240.0000	-138.5641	.22970-006
150.	60.	75.0000	129.9038	.41350-002	300.0000	173.2051	.55130-002
150.	45.	106.0660	106.0660	.33760-002	212.1320	212.1320	.67520-002
150.	30.	129.9038	75.0000	.23870-002	173.2051	300.0000	.95490-002
150.	15.	144.8889	38.8229	.12360-002	155.2914	579.5555	.18450-001
150.	0.	150.0000	.0000	.00000 000	150.0000	1.0000	.31830 046
150.	-15.	144.8889	-38.8229	.81990-006	155.2914	-579.5555	.54920-007
150.	-30.	129.9038	-75.0000	.42440-005	173.2051	-300.0000	.10610-006
150.	-45.	106.0660	-106.0660	.30010-006	212.1320	-212.1320	.15010-006
150.	-60.	75.0000	-129.9038	.24500-006	300.0000	-173.2051	.18380-006

TABLE IC

LOAD CALCULATIONS FOR NEUTRON AMPLIFIER
FREQUENCY = 5500.

ZMAG	ANG	RS	XS	LS OR CS	RP	XP	LP OR CP
15.	60.	7.5000	12.9904	.37590-003	30.0000	17.3205	.50120-003
15.	45.	10.6066	10.6066	.30690-003	21.2132	21.2132	.61390-003
15.	30.	12.9904	7.5000	.21700-003	17.3205	30.0000	.86810-003
15.	15.	14.4889	3.8823	.11230-003	15.5291	57.9555	.16770-002
15.	0.	15.0000	.0000	.00000 000	15.0000	1.0000	.28940 006
15.	-15.	14.4889	-3.8823	.74540-005	15.5291	-57.9555	.49930-006
15.	-30.	12.9904	-7.5000	.38580-005	17.3205	-30.0000	.96460-006
15.	-45.	10.6066	-10.6066	.27280-005	21.2132	-21.2132	.13640-005
15.	-60.	7.5000	-12.9904	.22280-005	30.0000	-17.3205	.16710-005
50.	60.	25.0000	43.3013	.12530-002	100.0000	57.7350	.16710-002
50.	45.	35.3553	35.3553	.10230-002	70.7107	70.7107	.20460-002
50.	30.	43.3013	25.0000	.72340-003	57.7350	100.0000	.28940-002
50.	15.	48.2963	12.9410	.37450-003	51.7638	193.1852	.55900-002
50.	0.	50.0000	.0000	.00000 000	50.0000	1.0000	.28940 006
50.	-15.	48.2963	-12.9410	.22360-005	51.7638	-193.1852	.14980-006
50.	-30.	43.3013	-25.0000	.11570-005	57.7350	-100.0000	.28940-006
50.	-45.	35.3553	-35.3553	.81850-006	70.7107	-70.7107	.40920-006
50.	-60.	25.0000	-43.3013	.66830-006	100.0000	-57.7350	.50130-006
80.	60.	40.0000	69.2820	.20050-002	160.0000	92.3760	.26730-002
80.	45.	56.5685	56.5685	.16370-002	113.1371	113.1371	.32740-002
80.	30.	69.2820	40.0000	.11570-002	92.3760	160.0000	.46300-002
80.	15.	77.2741	20.7055	.59930-003	82.8221	309.0963	.89440-002
80.	0.	80.0000	.0000	.00000 000	80.0000	1.0000	.28940 006
80.	-15.	77.2741	-20.7055	.13980-005	82.8221	-309.0963	.93620-007
80.	-30.	69.2820	-40.0000	.72340-006	92.3760	-160.0000	.18080-006
80.	-45.	56.5685	-56.5685	.51150-006	113.1371	-113.1371	.25590-006
80.	-60.	40.0000	-69.2820	.41770-006	160.0000	-92.3760	.31330-006
120.	60.	60.0000	103.9230	.30070-002	240.0000	138.5641	.40100-002
120.	45.	84.8528	84.8528	.24550-002	169.7056	169.7056	.49110-002
120.	30.	103.9230	60.0000	.17360-002	138.5641	240.0000	.69450-002
120.	15.	115.9111	31.0583	.89870-003	124.2331	463.6444	.13420-001
120.	0.	120.0000	.0000	.00000 000	120.0000	1.0000	.28940 006
120.	-15.	115.9111	-31.0583	.93170-006	124.2331	-463.6444	.62410-007
120.	-30.	103.9230	-60.0000	.48230-006	138.5641	-240.0000	.12060-006
120.	-45.	84.8528	-84.8528	.34100-006	169.7056	-169.7056	.17050-006
120.	-60.	60.0000	-103.9230	.27840-006	240.0000	-138.5641	.20880-006
150.	60.	75.0000	129.9038	.37590-002	300.0000	173.2051	.50130-002
150.	45.	106.0660	106.0660	.30690-002	212.1320	212.1320	.61390-002
150.	30.	129.9038	75.0000	.21700-002	173.2051	300.0000	.86810-002
150.	15.	144.8889	38.8229	.11230-002	155.2914	579.5555	.16770-001
150.	0.	150.0000	.0000	.00000 000	150.0000	1.0000	.28940 006
150.	-15.	144.8889	-38.8229	.74540-006	155.2914	-579.5555	.49930-007
150.	-30.	129.9038	-75.0000	.38580-006	173.2051	-300.0000	.96460-007
150.	-45.	106.0660	-106.0660	.27280-006	212.1320	-212.1320	.13640-006
150.	-60.	75.0000	-129.9038	.22280-006	300.0000	-173.2051	.16710-006

Our output power measurements then are essentially for the fundamental frequency component only, as all harmonic levels are down at least 26 dB below the fundamental after filtering.

The following set of three curves, Figs. (2), (3) and (4) show the output powers for the aforementioned loads and frequencies for maximum drive levels.

There is generally good agreement with shape and magnitude of our curves with those of the manufacturer. Where there are differences it is usually where the manufacturers curves deviate from the general curve shape. This could be due partly to the fact that the manufacturer used a thermocouple type detector for voltage and current output measurements which made his power calculations read for total power out, including the power contained in the harmonics of the distorted output signals, whereas our measurements are for the power contained in the fundamental frequency component only.

These curves can be compared directly with those published by the manufacturer in his final development report mentioned earlier.

5.2 DC Input Power

The DC input power to the Neotron tube as defined here is the "steady state" DC anode voltage, described in an earlier section, times the average value of the pulsating anode current. The anode current is a series of current pulses resembling the positive portion of a sinusoid with some distortion. See Fig. (5).

The anode current flows for slightly less than 180° of each positive half cycle of the driver output voltage. See Fig. (6). This picture is of a four cycle pulse with the amplifier loaded with 50 ohms non-reactive load at 5000 Hz and shows our substitute driver output voltage and the anode current wave form superimposed. The complete undistorted sine wave is the driver output and the somewhat distorted half wave form with the greater amplitude is the anode current. It can be seen that the anode current is on for slightly less than one half of the complete cycle. The percentage of conduction time seems to decrease slightly with high power levels as compared to lower drive levels.

Measurements were made at 5000 Hz for loads of 15 ohms, 50 ohms, 80 ohms, 120 ohms and 150 ohms magnitude with phase angles of zero degrees and $\pm$ 60 degrees.

The DC anode voltage was set at 5400 volts at steady state. However, due to the plate voltage regulation described before, there was a 5000 Hz ripple of about 1% of the DC level riding on the DC. This small ripple was not considered in the power input calculations.

The DC input power curves are shown in Fig. (3) with their corresponding output powers.

Our first definition of the Neotron anode DC input power was erroneously based on the product of the DC anode voltage and the true-rms value of the anode current and our measurements were made accordingly. A so called true-rms voltmeter and a one ohm resistor were used to measure the anode current. There were actually two errors made. First in the definition of the anode input power and second in interpreting the output of the true-rms voltmeter.

The discovery of the errors was not made until after the equipment setup was disassembled and the amplifiers no longer available for further measurements. Consequently, we had to use the information available to obtain a correction for the true-rms voltmeter reading in order to calculate the average anode current.

To get a correction figure we had to first make certain that we understood the output of the "true-rms" voltmeter. A careful study, after the fact, of the operation of the voltmeter shows that its indication is proportional to the rms deviation about the average of the impressed waveform and does not take into account the DC component of the waveform.

With this knowledge of the meter operation, we first calculated what the meter should read for an input of a "standard" type waveform which was similar to the current pulse. We naturally chose a half-wave rectified sine wave. This calculation is presented below.

$$V_{rms} = \left(\frac{1}{T}\int_0^T \Big(f(t)\Big)^2 dt\right)^{1/2}$$

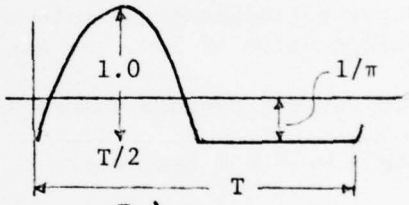

$$= \left(\frac{1}{T}\left[\int_0^{T/2} (\sin \omega t - 1/\pi)^2 dt + \int_{T/2}^{T} (-1/\pi)^2 \, dt\right]\right)^{1/2}$$

$$= \left\{\frac{1}{T}\left[\frac{1}{2\omega}\Big(\omega t - \sin \omega t \cos \omega t\Big) + \frac{2}{\pi\omega}\cos \omega t + \frac{t}{\omega^2}\right]_0^{T/2} + \frac{1}{T}\left[\frac{t}{\pi^2}\right]_{T/2}^{T}\right\}^{1/2}$$

= 0.386 of the peak value of the input

Where $\omega = \frac{2\pi}{T}$

An actual measurement of a half-wave rectified sine wave signal using the "true-rms" voltmeter yielded a meter indication of 0.392 of the peak value of the input. The same result was obtained for the same measurement using another "identical" meter of the same model. This close agreement between theory and experiment gave us confidence that we understood the operation of the meter.

Armed with this information, we proceeded to calculate a correction for the output of the "true-rms" voltmeter to give us the peak value of any unbalanced waveform such as the half-wave rectified sine wave.

If Vpk is the peak value of the voltage pulse and Vrms meter is the meter indication, then

$$\frac{\text{Vpk}}{\text{Vrms meter}} = \frac{1}{0.392} = 2.57 = \text{K}$$

then Vpk = K Vrms meter.

With this information, we can calculate the peak value of all of our anode current measurements where

Ipk = K Vrms meter

If we assume that the anode current pulse is the same shape as a half-wave rectified sine wave then we know that for a true hafl-wave the average value

$$\text{I avg} = \frac{1}{\pi} \text{ peak value}$$

However a graphical analysis of the current pulse train shows that instead of an average value of $1/\pi$, the actual average value was about 0.28.

Therefore our average values of anode current can be calculated as

I avg = 0.28 K I rms meter

= (0.28)(2.57) I rms meter

These average values of anode current are used in the anode DC input power curves of Fig. (3) and the DC input powers of Table II.

Our anode input power curves for the one frequency and range of loads that we ran are quite comparable in magnitude to the manufacturers curves but the shape as a function of load phase angle is somewhat different but not drastically so.

To actually measure the average value of the anode current pulses, an instrument which is capable of measuring the DC value of the pulse train is needed. A DC coupled low pass filter for instance could do the job.

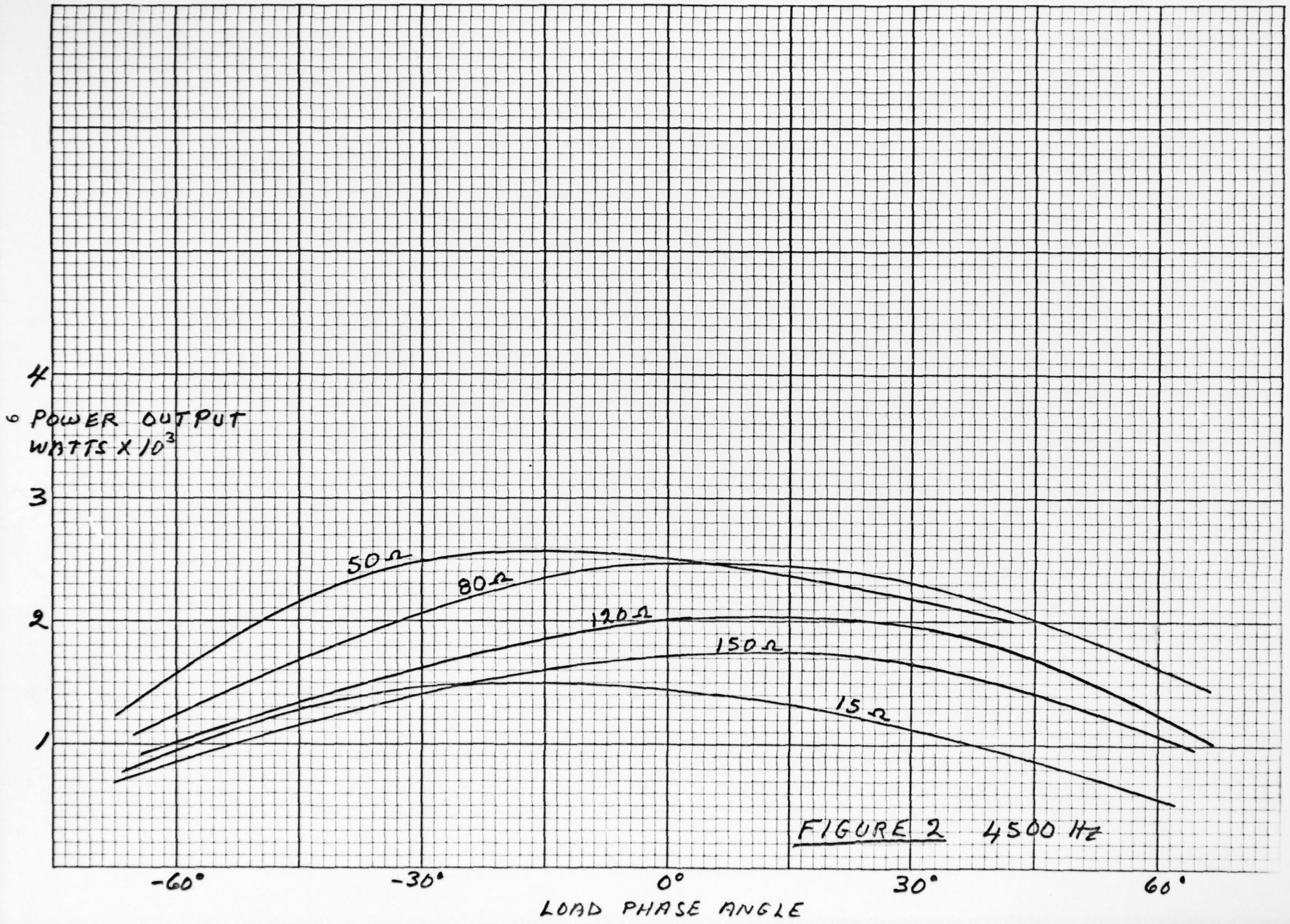

FIGURE 2 4500 Hz

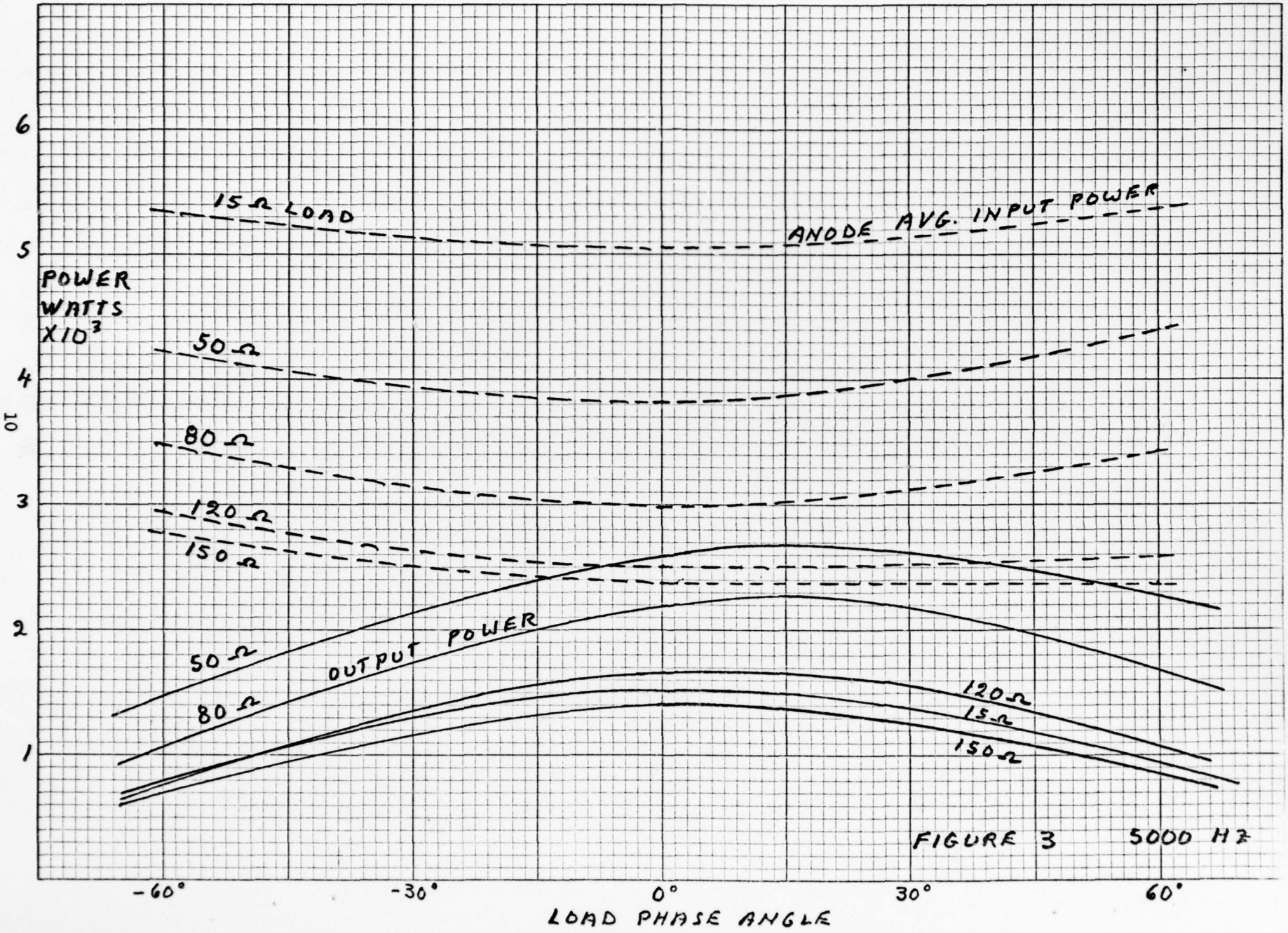

FIGURE 3 5000 HZ

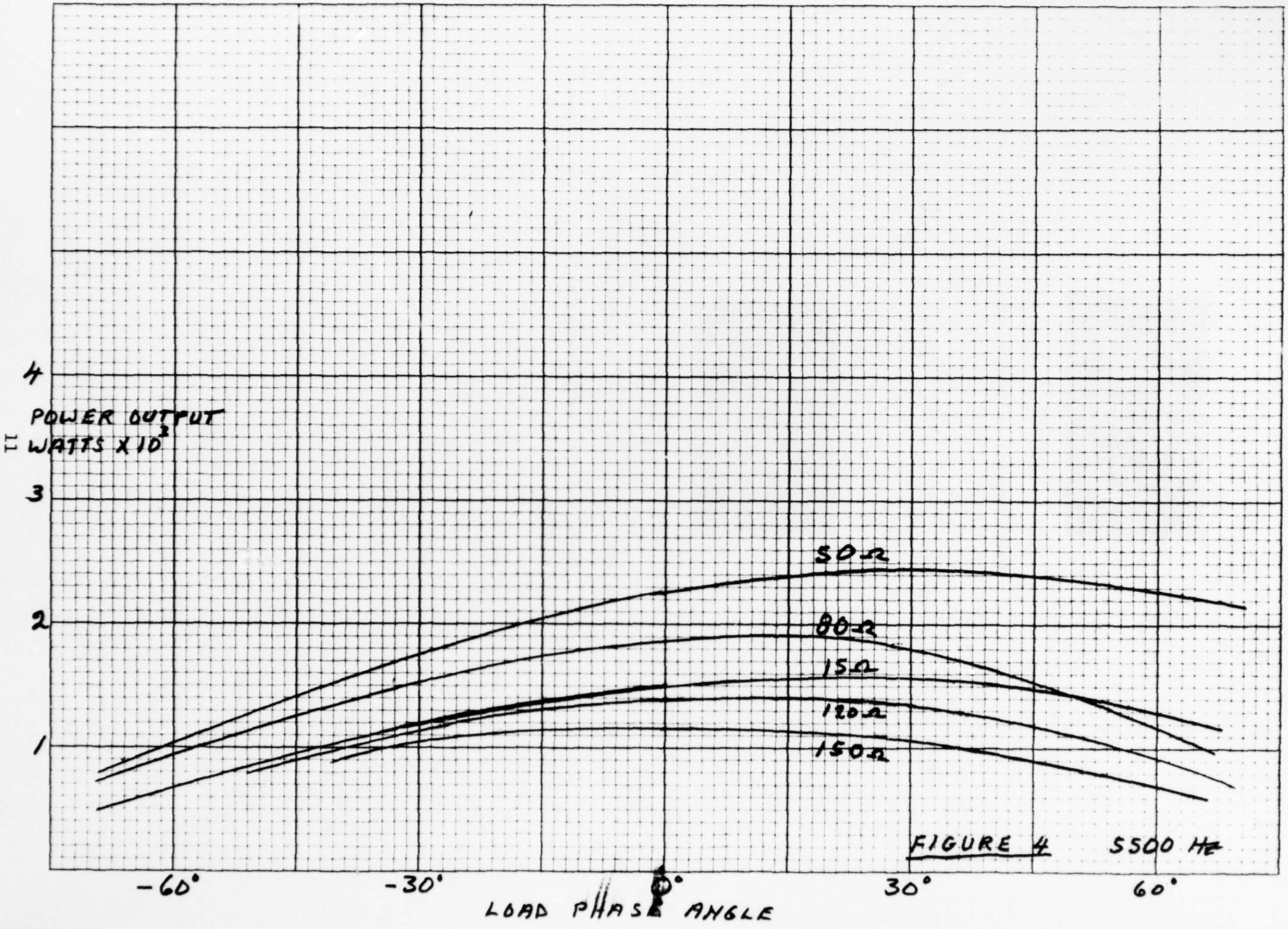

FIGURE 4 5500 Hz

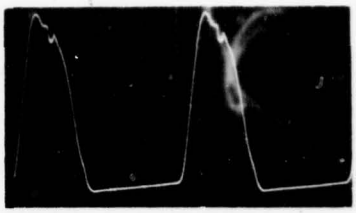

FIGURE 5

Anode Current Individual Cycle

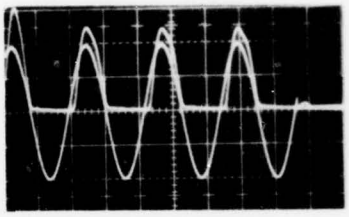

FIGURE 6

Driver Output Voltage (complete cycles)
and
Anode Current (positive pulses)

The above discussion concerns only the anode input power. The total input power to the module would include the anode input power plus the total power consumed in the heater filaments, the bias power and driver power. Then add to this the loss in the bias, driver and anode power supplies themselves. Thus the overall efficiency is something less than that shown in Table II and would depend partly upon the type and efficiency of the power supplies used.

The input powers, output powers, and efficiencies for specific loads at 5000 Hz are shown in Table II below.

TABLE II

LOAD OHMS	ANGLE	INPUT POWER WATTS	OUTPUT POWER WATTS	EFFICIENCY %
15	- 60°	5346	800	15
15	0°	5052	1510	30
15	+ 60°	5375	900	17
50	- 60°	4224	1300	31
50	0°	3814	2530	66
50	+ 60°	4397	2240	51
80	- 60°	3482	1060	30
80	0°	2979	2100	70
80	+ 60°	3432	1660	48
120	- 60°	2943	780	27
120	0°	2504	1630	65
120	+ 60°	2591	1040	40
150	- 60°	2785	700	25
150	0°	2382	1360	57
150	+ 60°	2389	860	36

5.3 Waveform Distortion

The output current and voltage waveforms are distorted. The amount of distortion and the shape of the waveforms depend upon the magnitude and phase angle of the load. The small change in frequency from 5000 Hz to 4500 Hz or 5500 Hz causes little change in the distortion level and generally speaking it is not a function of drive level.

Harmonic analysis was made of the output current and voltage waveforms at full power output at 5000 Hz for the load conditions of 15 ohms, 50 ohms and 150 ohms magnitude and zero degrees and $\pm$ 60 degrees phase angle.

The amplitude of all harmonics, out to 100 kHz, relative to the fundamental frequency amplitude are shown for the specific loads in the following set of pictures (Figs. 7, 8 & 9). Corresponding pictures of the actual voltage and current waveforms are also shown.

In the harmonic amplitude pictures the X axis shows the frequency out to 100 kHz at 10 kHz/division with the zero (DC) frequency marker on the left and the fundamental frequency and each subsequent harmonic at each half division. The amplitude scale is 10 dB/division with the fundamental at full scale (0dB) and the harmonic amplitudes at the indicated dB level below the fundamental.

In the output waveform pictures, the voltage and current waveforms are superimposed with the voltage always the larger of the two waveforms shown in each picture.

The per cent total harmonic distortion for each load condition was calculated from the harmonic pictures and the equation

$$\% D_T = \frac{\sqrt{\Sigma(\text{harmonics})^2}}{\text{fundamental}} \times 100.$$

These distortion measurements consider only the magnitude of the harmonics. No attempt was made to take into account the phase relationships of the harmonics.

The input signal waveforms were examined in the same way. The signal generator output harmonic analysis is shown in Fig. (10). This shows that all harmonics are at least 60 dB down from the fundamental. The harmonic output of the module drive with about 5% distortion for full power input is shown in Fig. (11). The driver voltage output waveform for 200 mv. input signal Fig. (12a) and for 500 mv. input signal Fig. (12b) are also shown. This shows the driver output with about the same amount of distortion for any input signal level.

Consideration was next given to substitution of another driver with a "clean" output for the built-in driver. Fig. (13a, b,c) shows the substitute driver output voltage (upper waveform in all cases) and three examples of corresponding output current waveforms for loads of 50 ohms zero degrees, 15 ohms zero degrees and 15 ohms at -65 degrees phase angles at full power out.

These indicate that with a clean driver, distortion still appears in the output current. At lower levels under the same conditions the distortion appears about the same.

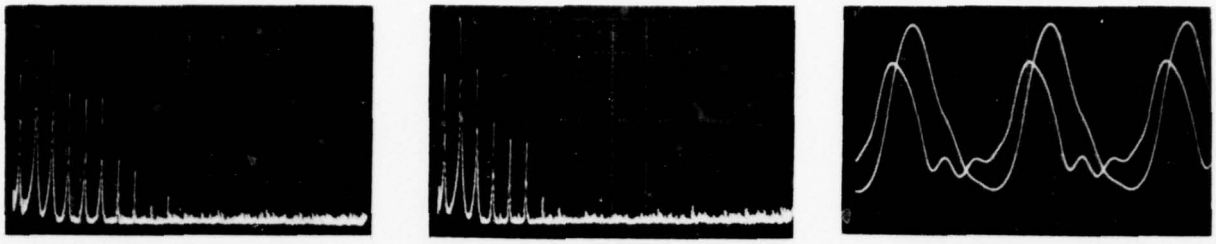

I_o 53% E_o 18% E_o & I_o WAVEFORMS

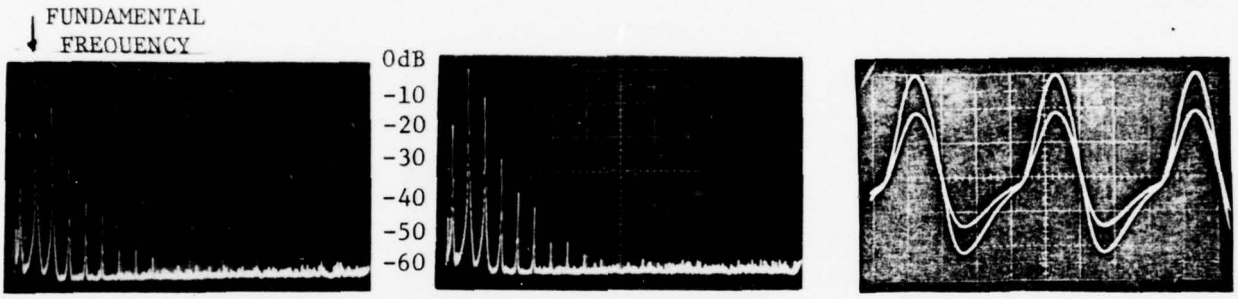

I_o 42% E_o 42% E_o & I_o (E_o is the greater magnitude)

15 Ω 0° LOAD

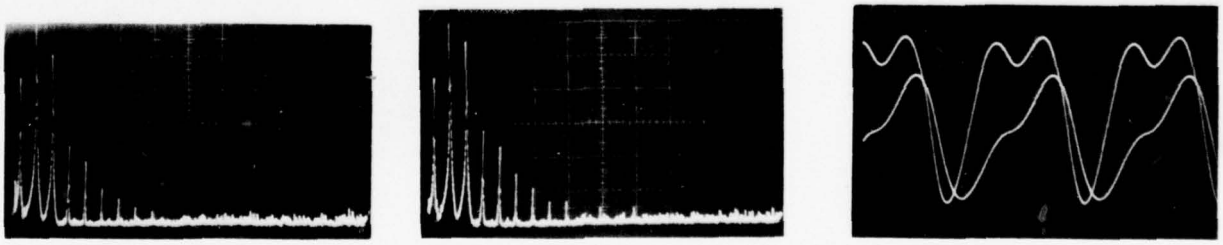

I_o 30% E_o 50% E_o & I_o

15 Ω +60° LOAD

FIGURE 7. Output voltage and current waveforms, harmonic levels and percent distortion for 15 ohm loads at 0° & ±60° phase.

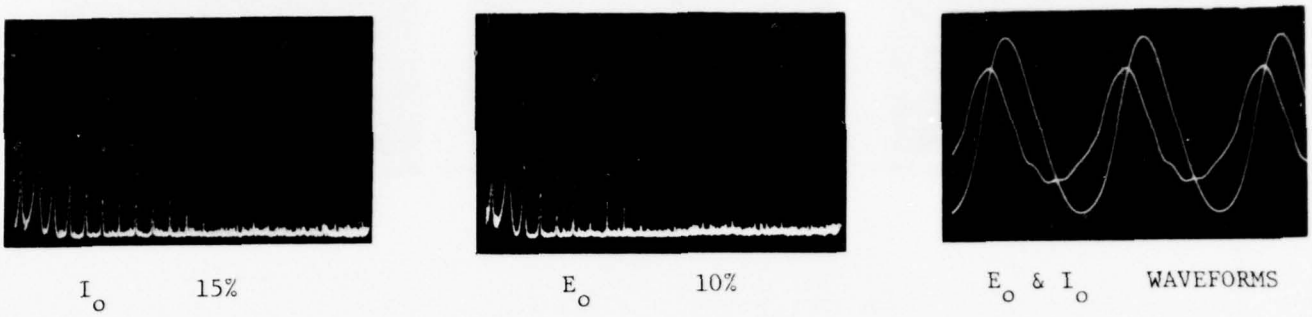

I_o 15% E_o 10% E_o & I_o WAVEFORMS

50 Ω -60° LOAD

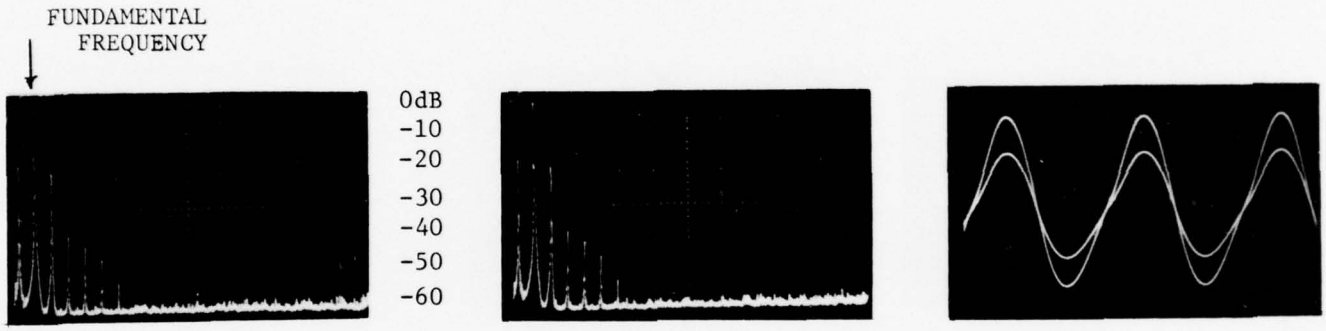

I_o 13% E_o 13% E_o & I_o
(E_o is the greater magnitude)

50 Ω 0° LOAD

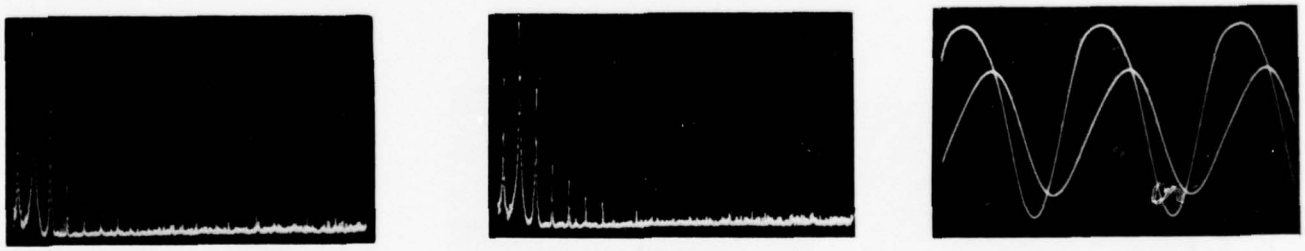

I_o 7% E_o 13% E_o & I_o

50 Ω +60° LOAD

FIGURE 8. Output voltage and current waveforms, harmonic levels and per cent distortion for 50 ohm loads at 0° & ±60° phase.

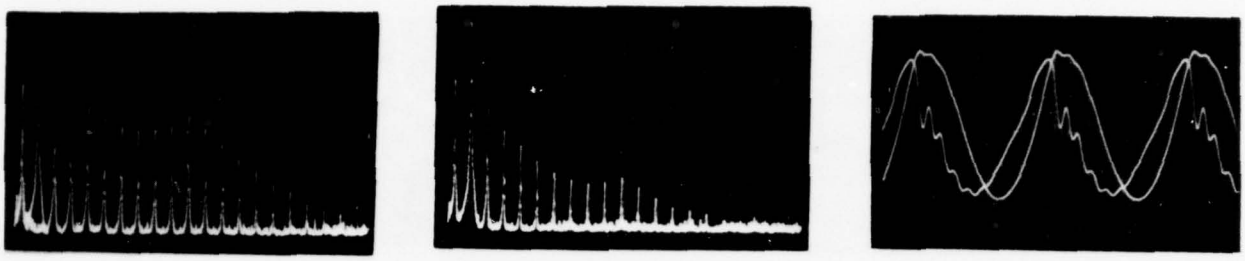

I_o 20% E_o 6% E_o & I_o WAVEFORMS

150 Ω -60° LOAD

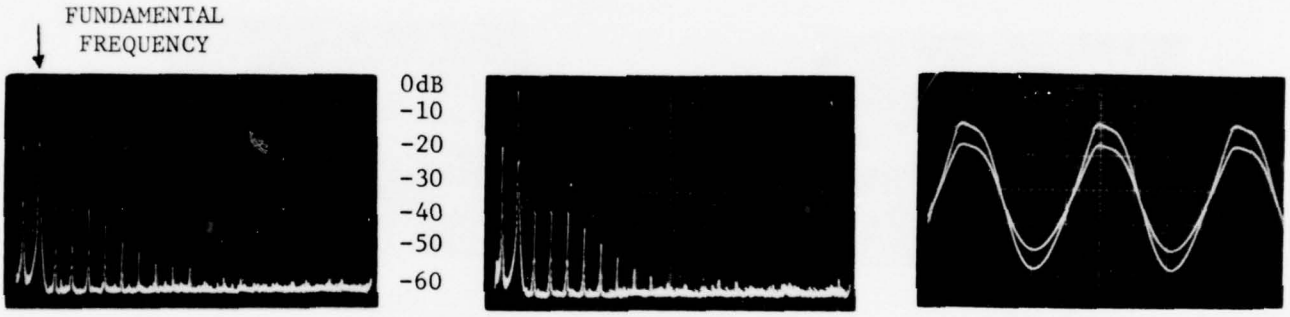

I_o 3% E_o 3% E_o & I_o
(E_o is the greater magnitude)

150 Ω 0° LOAD

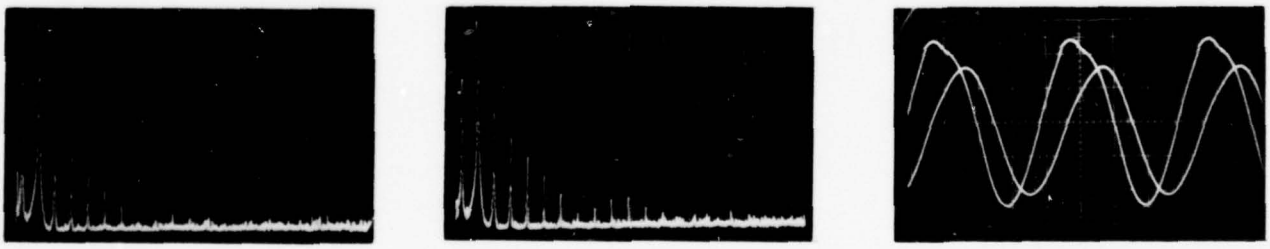

I_o 3% E_o 5% E_o & I_o

150 Ω +60° LOAD

FIGURE 9. Output voltage and current waveforms, harmonic levels and per cent distortion for 150 ohm loads at 0° & ± 60° phase.

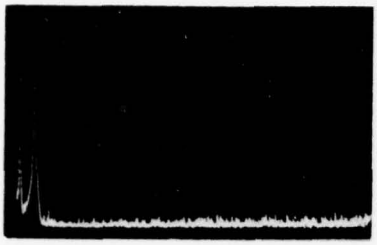

< 0.1%

FIGURE 10.

Signal Generator Harmonic Analysis

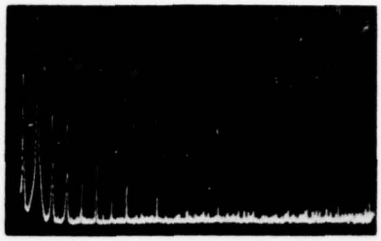

5%

FIGURE 11.

Module Driver Output Harmonic Analysis

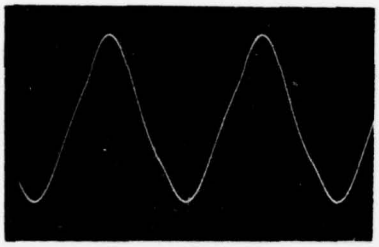

FIGURE 12a.

Module Driver Output for 200 mv. input signal

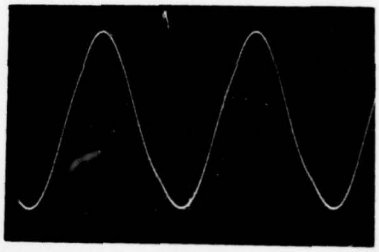

FIGURE 12b.

Module Driver Output for 500 mv. input dignal

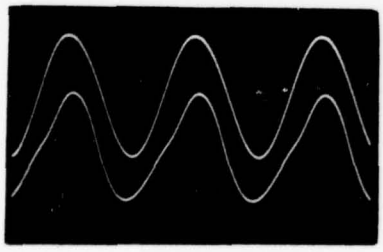

(a) 50 Ω 0° LOAD

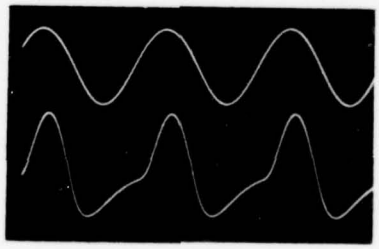

(b) 15 Ω 0° LOAD

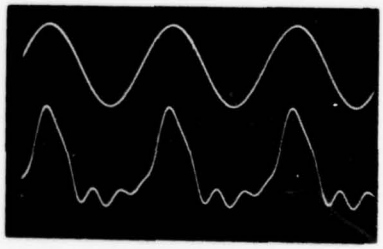

(c) 15 Ω -60° LOAD

FIGURE 13. I_o (bottom waveform) for three loads using a clean substitute driver output voltage (upper waveform).

5.4 Linearity

The linearity of the power output as a function of input signal level was measured. For this test the driver gain control was again set for 2500 watts output at 5000 Hz with a 50 ohm non-reactive load for 500 mv. rms input signal level. The function of the driver gain control was discussed earlier. Output powers were calculated for input levels ranging from 500 mv. rms down to 150 mv. rms. There was no amplifier output below about 125 mv. rms input signal level. Fig. (14) shows the decrease in power output in dB from full power output as a function of decrease in input signal level.

Another type of linearity was also measured. Input power and output power as a function of DC anode voltage for the load condition of 50 ohms non-reactive at 5000 Hz. The results are shown in Fig. (15). Our values and curve shape are much the same as those published by the manufacturer with the exception that our curve does not tend to flatten off at the top end. Note that the true rms input power curve scale is a factor of two greater than the output curve. Fig. (16) shows the waveforms of the driver output voltage, the anode current and the output current for the above load condition with anode voltages of 5400 V.DC and 1000 V.DC.

5.5 Phase Relationships Through the Amplifier and Settling Time From the Start of An Input Pulse

Time delay through the amplifier, that is, the phase relationship between the input signal source and output voltage and current is of interest for amplifier modeling as well as for a complete evaluation of the amplifier. Also of interest is the time required for the amplifier output to settle down to a steady state condition after the start of an input pulse.

Phase relationships between the input voltage as a reference and the output voltage and current were measured under steady state conditions during the high power measurements for output powers and are shown in Table III.

Though not directly related to this subject but included for general information the magnitudes of the output voltage and output current under the same conditions are shown in Table IV.

As was mentioned before, the anode current only flows on the positive portion of the driver output signal. Consequently if the start of the driver pulse is on some portion of the negative half cycle, plate current does not start to flow until some positive level on the driver signal is reached. Fig. (17) illustrates this. Fig. (17a & b) show the input signal (upper waveform in all four pictures) triggered on a negative portion of the cycle and the corresponding anode and output current waveforms showing no output until a positive level of input signal is reached on the next half cycle. Fig. (17c & d) show the input voltage triggered at a positive level and the corresponding anode and output currents starting with just a slight delay. This is for a 50-ohm non-reactive load at 5000 Hz. A phase coherent tone burst generator that could be triggered at any point on the cycle was used as the pulse generator for testing these conditions.

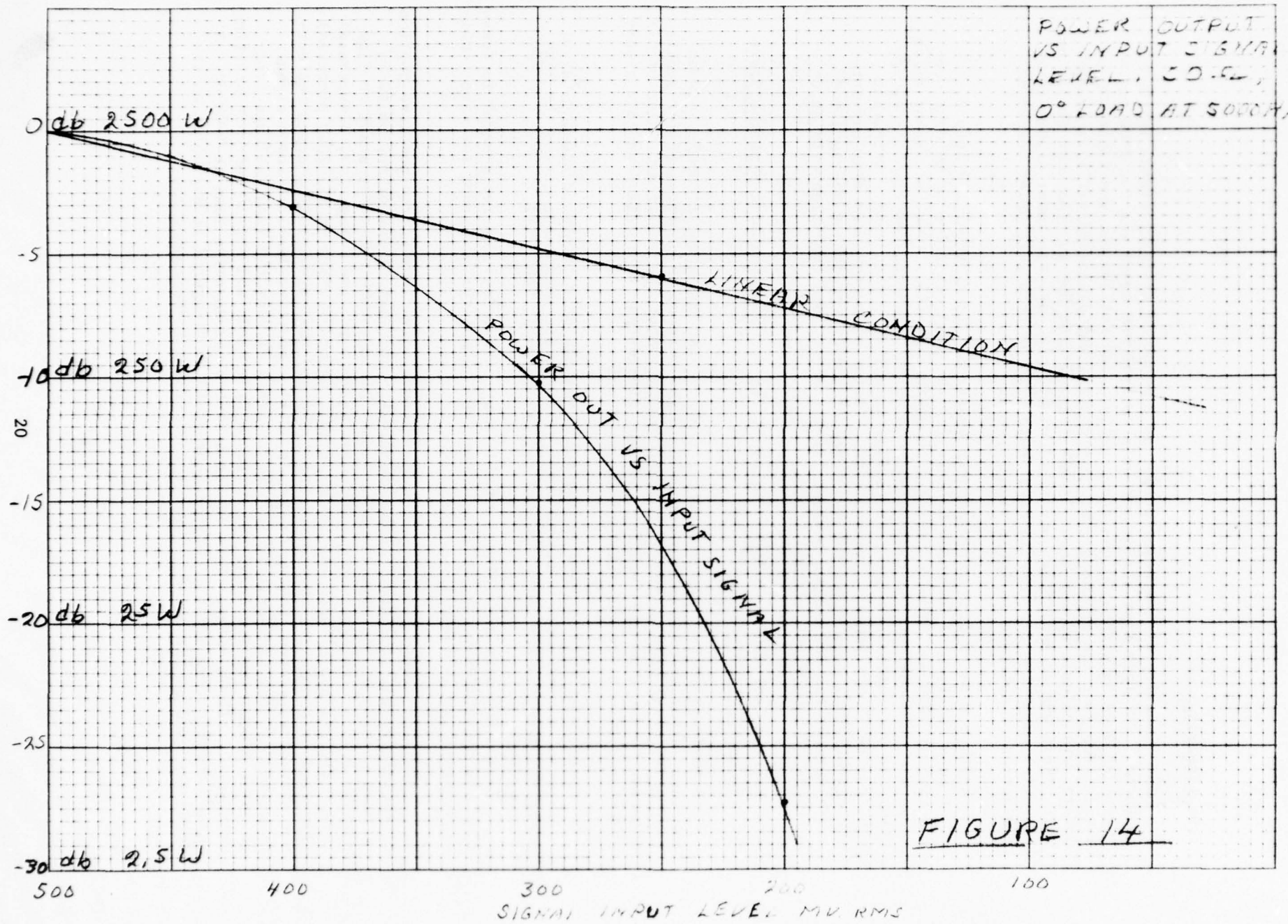

FIGURE 14

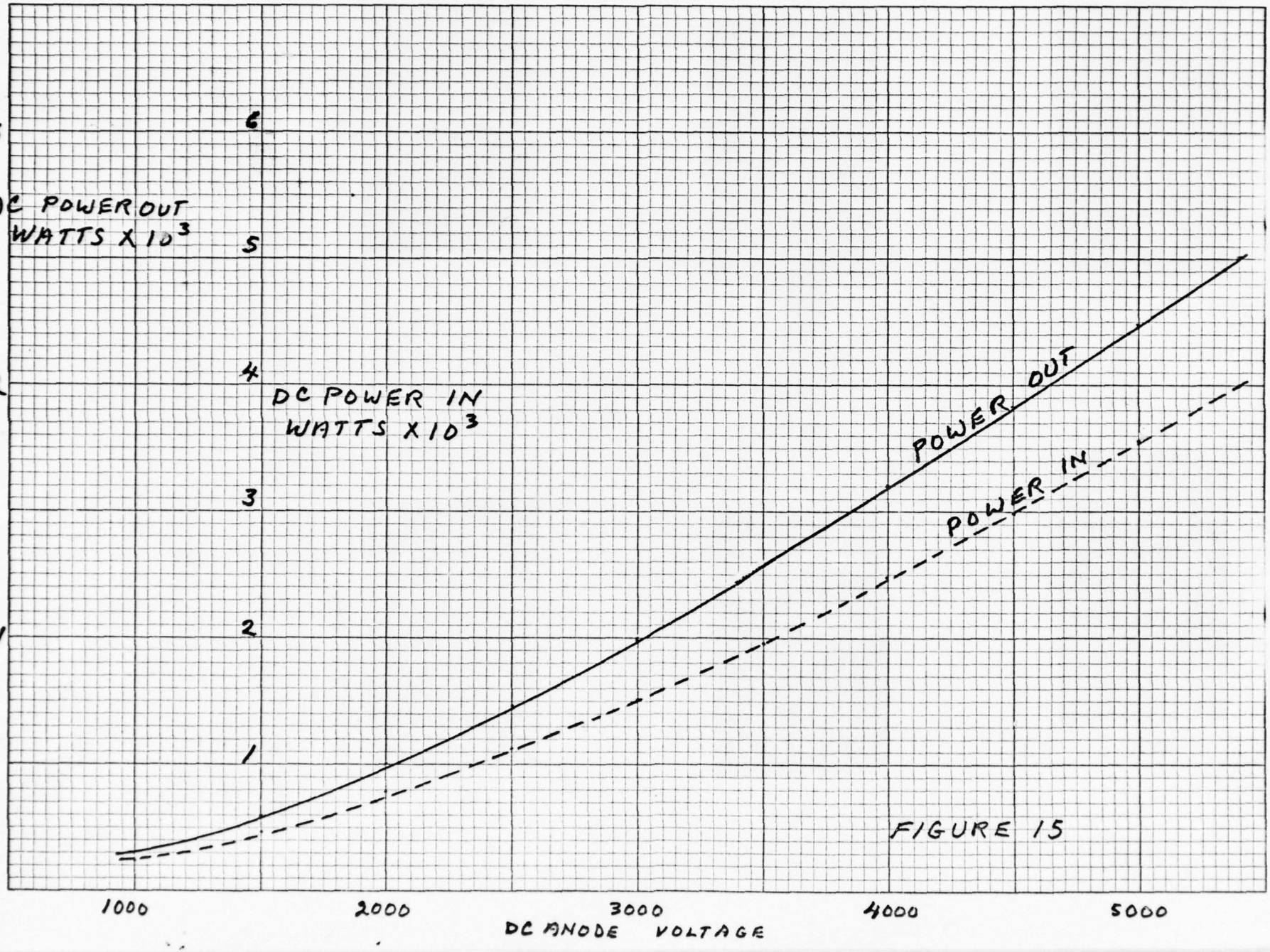

FIGURE 15

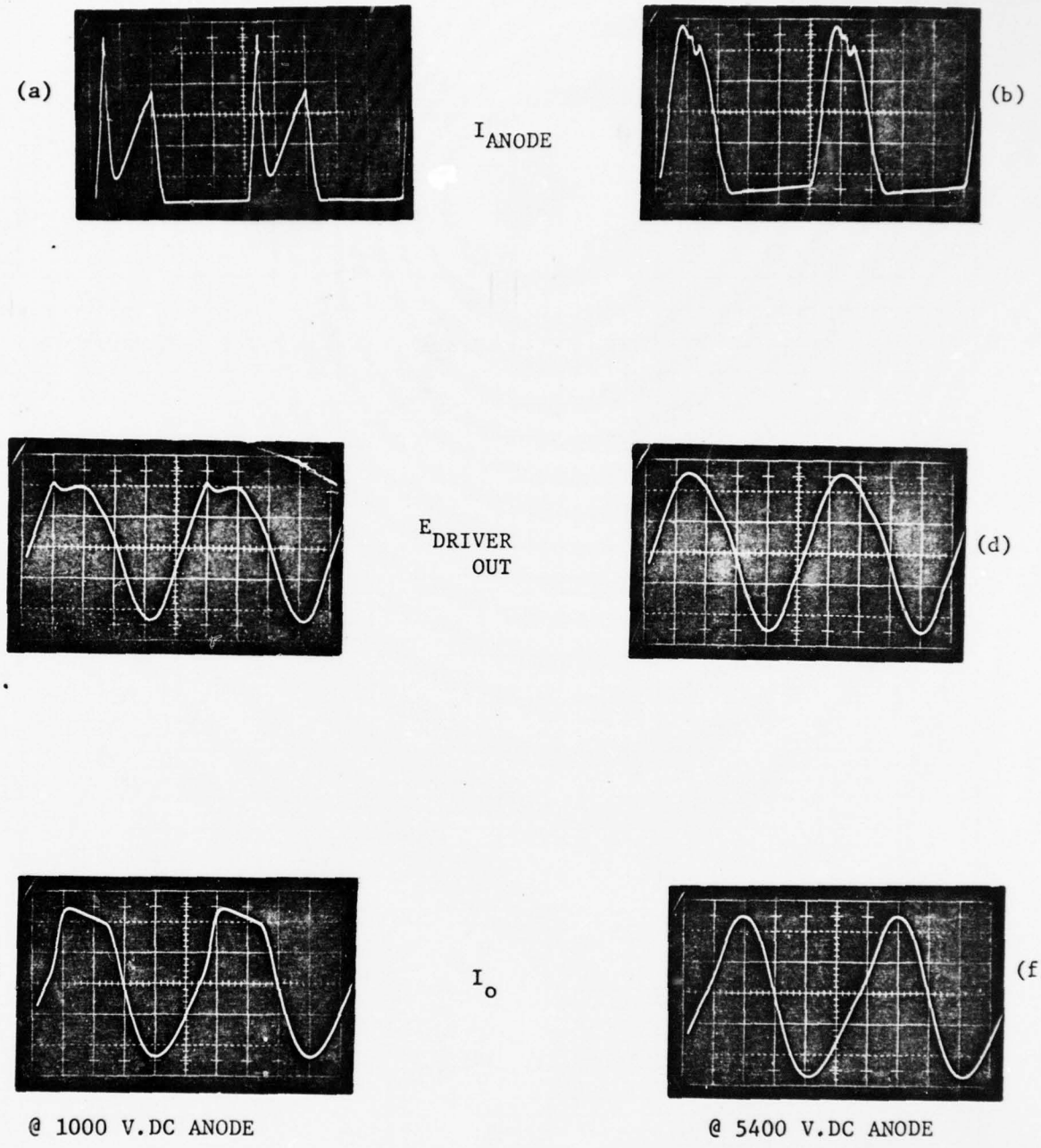

FIGURE 16. $E_{DRIVER\ OUT}$, I_{ANODE} and I_o waveforms as a function of anode voltage.

TABLE III

LOAD		4500 Hz		5000 Hz		5500 Hz	
Mag.	Angle	Angle E_o	Angle I_o	Angle E_o	Angle I_o	Angle E_o	Angle I_o
	- 60°	- 54°	6°	- 64°	- 4°	- 72°	- 12°
	- 30°	- 22°	8°	- 35°	- 5°	- 47°	- 17°
15 Ω	0°	5°	5°	- 6°	- 6°	- 18°	- 18°
	+ 30°	30°	0°	20°	- 10°	8°	- 22°
	+ 60°	54°	- 6°	47°	- 13°	36°	- 24°
	- 60°	- 27°	33°	- 58°	2°	- 72°	- 12°
	- 30°	- 10°	20°	- 34°	- 4°	- 54°	- 24°
50 Ω	0°	12°	12°	- 12°	- 12°	- 34°	- 34°
	+ 30°	31°	- 1°	11°	- 19°	- 16°	- 46°
	+ 60°	52°	- 8°	32°	- 28°	14°	- 46°
	- 60°	- 12°	48°	- 44°	16°	- 71°	- 11°
	- 30°	- 2°	28°	- 30°	0°	- 56°	- 26°
80 Ω	0°	15°	15°	- 14°	- 14°	- 40°	- 40°
	+ 30°	33°	3°	2°	- 28°	- 25°	- 55°
	+ 60°	51°	- 9°	16°	- 44°	- 15°	- 75°
	- 60°	- 3°	- 57°	-33°	27°	- 64°	- 4°
	- 30°	3°	33°	- 27°	3°	- 54°	- 24°
120 Ω	0°	17°	17°	- 14°	- 14°	- 42°	- 42°
	+ 30°	31°	1°	3°	- 33°	- 31°	- 61°
	+ 60°	47°	- 13°	7°	- 53°	- 21°	- 81°
	- 60°	1°	61°	- 30°	30°	- 61°	- 1°
	- 30°	6°	36°	- 25°	5°	- 51°	- 21°
150 Ω	0°	16°	16°	- 15°	- 15°	- 42°	- 42°
	+ 30°	30°	0°	- 6°	- 36°	- 33°	- 63°
	+ 60°	43°	- 17°	3°	- 57°	- 24°	- 84°

Phase angles of E_o and I_o relative to E_{in} as reference.

TABLE IV

LOAD		4500 Hz		5000 Hz		5500 Hz	
Mag.	Angle	$\|E_o\|$	$\|I_o\|$	$\|E_o\|$	$\|I_o\|$	$\|E_o\|$	$\|I_o\|$
	- 60°	167	11.5	156	10.5	142	9.78
	- 30°	158	10.3	151	10.1	141	9.69
15	0°	147	9.70	152	10.0	151	9.97
	30°	138	9.64	150	10.2	161	10.8
	60°	131	9.55	165	10.7	193	12.4
	- 60°	410	7.63	384	7.64	308	6.66
	- 30°	380	7.55	354	7.16	327	6.22
50	0°	352	6.97	359	7.11	337	6.74
	30°	350	7.28	388	7.77	379	7.45
	60°			472	8.75	459	10.9
	- 60°	454	5.33	423	5.26	384	5.18
	- 30°	436	5.43	403	5.06	378	4.93
80	0°	442	5.56	411	5.09	384	4.80
	30°	458	5.93	448	5.60	409	5.03
	60°	495	6.51	511	6.19	449	5.11
	- 60°	490	3.86	449	3.50	418	3.41
	- 30°	476	3.96	437	3.55	405	3.33
120	0°	491	4.10	443	3.67	408	3.41
	30°	517	4.39	467	3.88	428	3.59
	60°	545	4.47	511	4.03	461	3.83
	- 60°	505	3.37	457	3.28		
	- 30°	495	3.28	447	2.95	416	2.86
150	0°	506	3.38	455	3.02	416	2.79
	30°	534	3.60	474	3.09	432	2.86
	60°	573	3.83	515	3.36	460	3.08

Magnitudes of E_o (volts) and I_o (amps) rms.

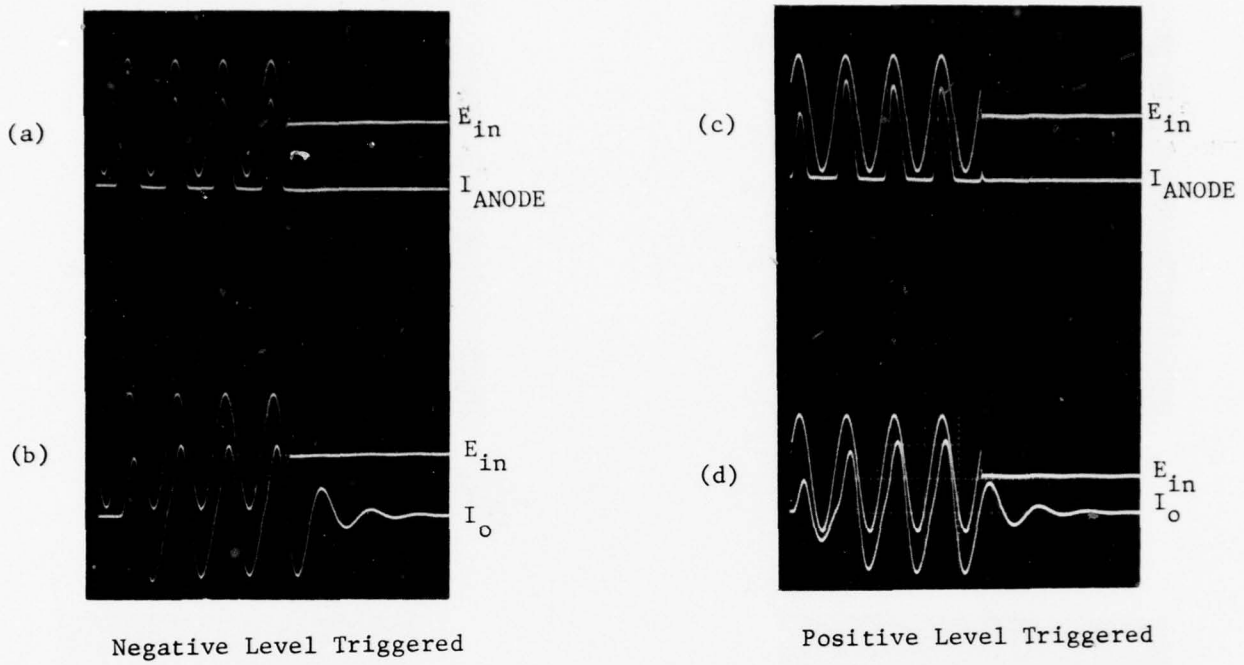

FIGURE 17. Anode current and output current waveforms as a function of driver pulse starting trigger level.

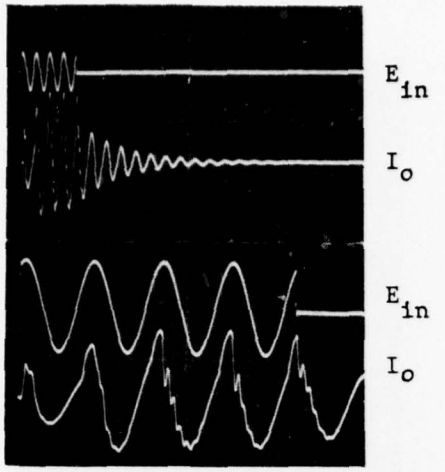

Positive Level Triggered

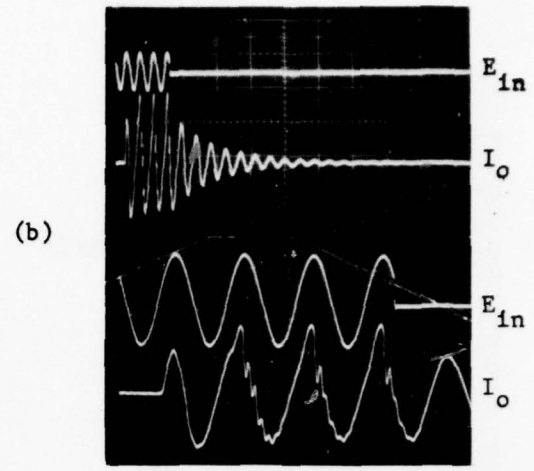

Negative Level Triggered

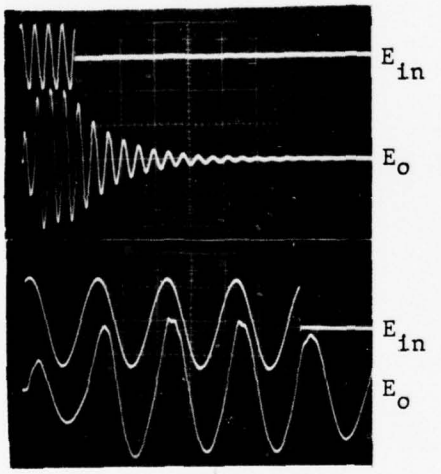

Positive Level Triggered

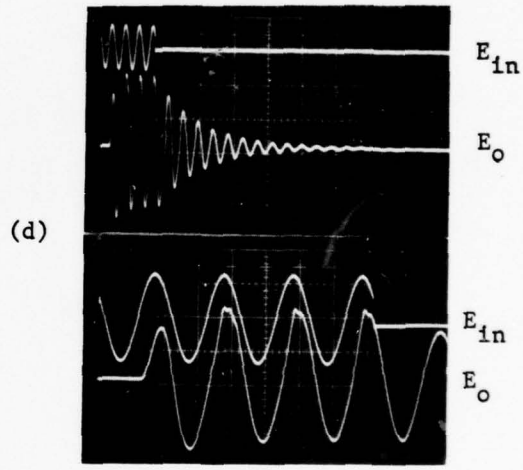

Negative Level Triggered

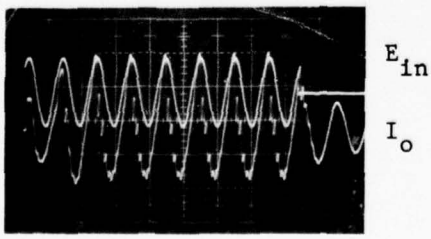

Positive Level Triggered

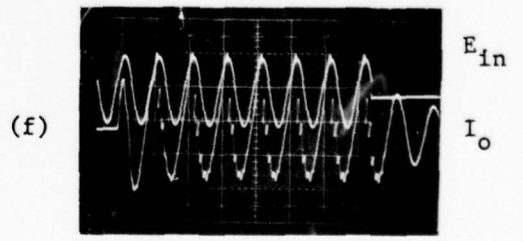

Negative Level Triggered

FIGURE 18. E_o and I_o settling time for 150 Ω -60° load at 5000 Hz.

Time delay then for the start of a pulse is roughly a function of the starting level of the first cycle of the start of the pulse plus the indicated steady state phase relationship.

The time required for the amplifier output to settle down to a steady state condition after the start of a pulse seems to be a function of the triggering level discussed above and also the load conditions on the amplifier. For example, Figs. (17b & d) show a four cycle pulse of the input voltage (upper waveform) and the output current for a 50-ohm non-reactive load at 5000 Hz. Fig. (17d) is triggered on the positive level and requires three to four cycles to settle down while Fig. (17b) is triggered on the negative level but the output settles down in about two cycles.

As another example, Fig. (18) shows waveforms for a load of 150 ohms at -60° at 5000 Hz. In all pairs of pictures the driver input voltage is the upper waveform. Figs. (18a & b) show a four cycle pulse of the input voltage and the output current. Figs. (18e & f) are the same thing as the lower half of (a & b) but using an eight cycle pulse. Fig. (18c & d) show the input voltage and output voltage for the same conditions of the current four cycle pulses. Figs. (18a, c & e) are positive triggered and (b, d & f) are negative triggered. The upper pictures in Figs. (18a, b, c & d) show a broad picture of the pulse and the lower picture shows the details of the four cycles.

From the upper pictures in Figs. (18a, b, c & d) it can be seen that under these load conditions the output does not settle down in less than four cycles. Close inspection of Fig. (18f) indicates that the output has just about settled down in amplitude and relative phase after about four cycles.

Figs. (17) and (18) show that the output "rings" for some time after the end of the pulse. Here again it is a function of the amplifier load.

5.6 Repeatability

Long term repeatability of measurements could not be established at better than about $\pm$ 2%. This did not come entirely from instrumentation which had a possible accumulative error of less than $\pm$ 1%.

Short term repeatability was well within the instrumentation error range.

A 50-ohm non-reactive load capable of dissipating 5 kilowatts of power was used as a reference load. Continued periodic measurements of this load, interspersed into the other measurement routine, gave a running check of the repeatability of measurements. No real trend in measurement anomaly could be found, just the random scatter of about $\pm$ 2%.

Measurements on several modules indicated a uniformity from module to module to be within the repeatability of our measurements.

6.0 Linear Amplifier Models

The second purpose for performing this experiment was to determine equivalent linear amplifier circuits or models for the amplifier under various load conditions at each frequency of interest. This is accomplished by using a Thevenin-Norton equivalent circuit linear amplifier computer data fit program developed in Code 601. This is a procedure whereby electronic measurements are made on a specific amplifier and then used as inputs for a computer program which will predict linear amplifier models from this data.

The procedure which is followed requires the selection of the signal frequency of the test and the range of loads with which the amplifier will be tested. The specific measurement made on the amplifier are the magnitudes of the input voltage, output current, output voltage and all possible combinations of the relative phase angles between these. This empirical data is then inputted into the computer program. The computer output gives both a Thevenin and a Norton equivalent circuit linear amplifier for this set of loads at this frequency. A separate pair of linear models is generated for each set of loads at each frequency. The equivalent linear amplifier circuits and the symbology used are shown in Fig. (19).

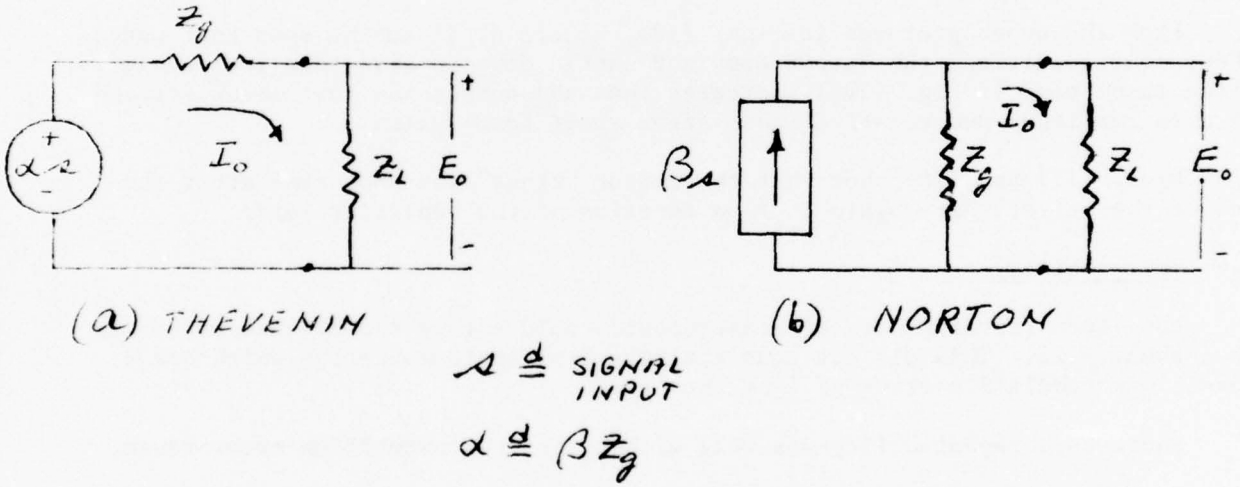

FIG. (19) Equivalent Linear Amplifier Circuits

The output also predicts the complex output voltage and current and the calculated power associated with each specific load condition for a given input signal level. Comparisons can then be made between the empirical data and the predicted data in all possible combinations. For the following amplifier tests we chose to calculate the percentage difference of the magnitudes and the difference in phase angle in degrees of the measured data from the corresponding predicted linear amplifier data for the output voltage, current and power.

The following curves and tables of linear amplifier data are based on the complete set of amplifier loads used for the power output measurements, namely magnitudes of 15, 50, 80, 120 and 150 ohms at phase angles of 0°, ±30° and ±60°. These were used at the three frequencies of 4500 Hz, 5000 Hz and 5500 Hz.

Table V shows the values of the computer predicted circuit components for each of the three test frequencies used.

TABLE V

FREQ	THEVENIN		NORTON	
	Z_g	αE_{in}	Z_g	βI_{in}
4500	61.7 /21.9°	680 + J310	75.7 /21.9°	11.0 + J0.658
5000	52.7 /-12.3°	634 - J209	67.2 /-12.3°	717 - J245
5000	43.4 /-41.6°	332 - J439	54.5 /-41.6°	10.9 - J2.58

Table VI shows the maximum difference between the measured and calculated values of voltage and current. It turns out that the percentage error and the difference in the angle is the same for both voltage and current at each individual load condition for each equivalent circuit.

TABLE VI

THEVENIN FIT			
	4500 Hz	5000 Hz	5500 Hz
Max. Mag. Error	-23%	+16%	+18%
Max. Angle Error	±9°	-15°	+15°
NORTON FIT			
	4500 Hz	5000 Hz	5500 Hz
Max. Mag. Error	-29%	-18%	+25%
Max. Angle Error	-7°	-11°	-10°

The following tables show how the measured output voltage or current data compares with the predicted data for all load conditions at the three frequencies. Curves are plotted for both magnitude percentage difference and angular difference vs magnitude of load for load phase angles of 0° and $\pm$60° for both Thevenin and Norton circuits.

TABLE VII - 4500 Hz

AMPLIFIER LOAD		MAGNITUDE DIFFERENCE IN %				PHASE DIFFERENCE IN DEGREES	
MAG.	ANGLE	POWER (NORT)	POWER (THEV)	E_o & I_o (NORT)	E_o & I_o (THEV)	E_o & I_o (NORT)	E_o & I_o (THEV)
15	- 60°	16	- 1	8	- 1	- 7	- 9
	- 30°	14	1	7	1	- 4	- 5
	0°	9	- 3	4	- 1	- 3	- 3
	30°	8	- 4	4	- 2	- 2	- 1
	60°	1	- 10	1	- 5	- 2	0
50	- 60°	- 16	- 18	- 8	- 9	- 3	- 7
	- 30°	6	4	3	2	- 4	- 6
	0°	7	6	3	3	0	0
	30°	16	14	7	6	2	3
	60°						
80	- 60°	- 37	- 33	- 21	- 18	0	- 4
	- 30°	- 16	- 13	- 8	- 7	- 2	- 4
	0°	3	6	2	- 3	0	0
	30°	17	21	8	10	4	6
	60°	27	30	12	14	6	9
120	- 60°						
	- 30°						
	0°	- 11	- 4	- 6	- 2	- 1	- 1
	30°	3	10	1	5	5	6
	60°	2	11	1	5	6	9
150	- 60°	- 49	- 41	- 29	- 23	0	- 2
	- 30°	- 34	- 26	- 19	- 14	- 3	- 4
	0°	- 17	- 11	- 10	- 6	- 2	- 2
	30°	- 7	2	- 4	1	2	3
	60°	- 2	8	- 1	4	5	7

Magnitude and phase angle comparisons of measured vs. predicted voltage, current and power.

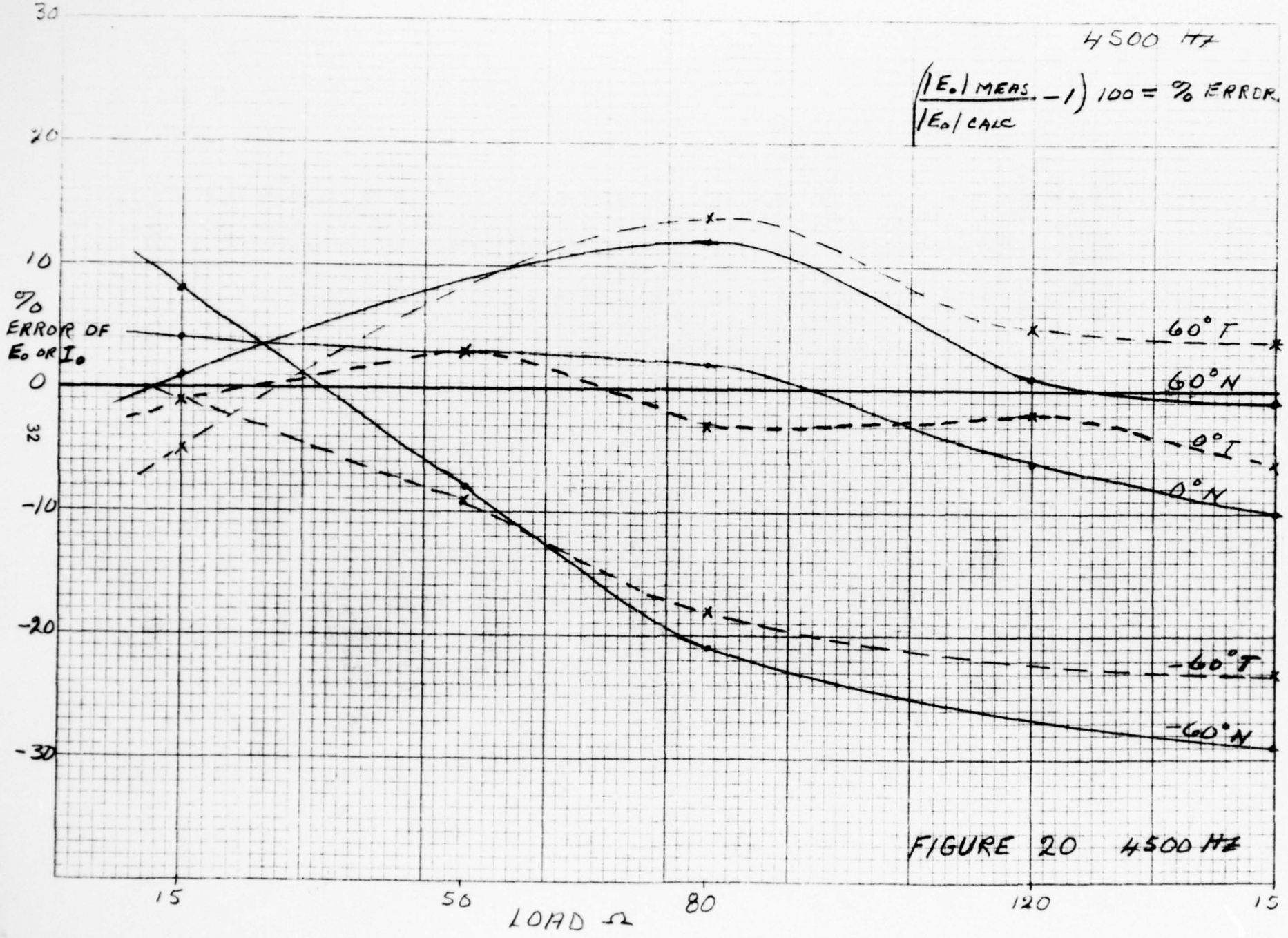

FIGURE 20 4500 Hz

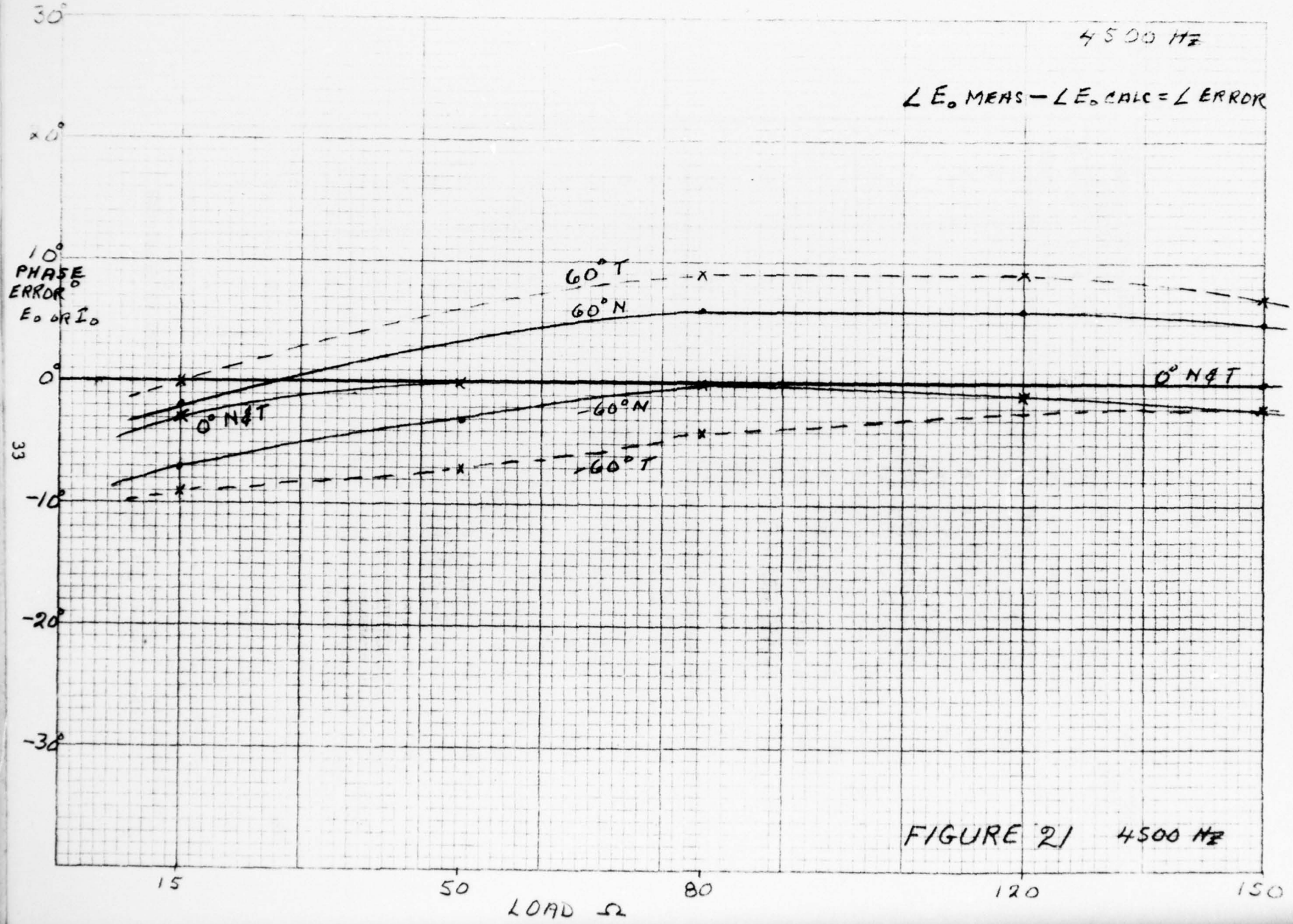

FIGURE 21 4500 HZ

TABLE VIII - 5000 Hz

AMPLIFIER LOAD		MAGNITUDE DIFFERENCE IN %				PHASE DIFFERENCE IN DEGREES	
Mag.	Angle	POWER (NORT)	POWER (THEV)	E_o & I_o (NORT)	E_o & I_o (THEV)	E_o & I_o (NORT)	E_o & I_o (THEV)
	- 60°	14.6	- 1.6	8	- 1	- 5	- 8
	- 30°	17.8	2.8	9	1	- 2	- 3
15	0°	18.2	3.4	9	1	2	2
	30°	13.3	- 2.3	6	- 1	4	5
	60°	10.7	- 6.2	5	- 4	6	8
	- 60°	16.0	14.5	8	7	- 11	- 15
	- 30°	17.6	16.3	8	8	- 5	- 7
50	0°	20.4	19.4	9	9	0	0
	30°	25.6	23.9	12	11	5	7
	60°	34.7	33.8	16	16	10	14
	- 60°	- 12.8	- 7.9	- 7	- 4	- 4	- 8
	- 30°	- 6.4	- 1.8	- 4	- 1	- 4	- 5
80	0°	- 2.2	2.7	- 1	1	0	0
	30°	4.4	9.9	2	5	3	4
	60°	1.7	8.9	1	4	3	7
	- 60°	- 30.6	- 22.2	- 17	- 12	2	- 1
	- 30°	- 21.5	- 13.5	- 11	- 7	- 1	- 2
120	0°	- 18.0	- 9.9	- 9	- 6	0	0
	30°	- 19.7	- 9.8	- 10	- 5	1	3
	60°	- 25.6	- 14.9	- 14	- 8	2	5
	- 60°	- 32.8	- 23.7	- 18	- 13	3	- 1
	- 30°	- 28.9	- 20.9	- 16	- 10	0	- 1
150	0°	- 25.4	- 16.1	- 13	- 8	0	0
	30°	- 27.2	- 17.1	- 15	- 9	0	1
	60°	- 32.0	- 20.3	- 17	- 11	2	5

Magnitude and phase angle comparisons of measured vs predicted voltage, current and power.

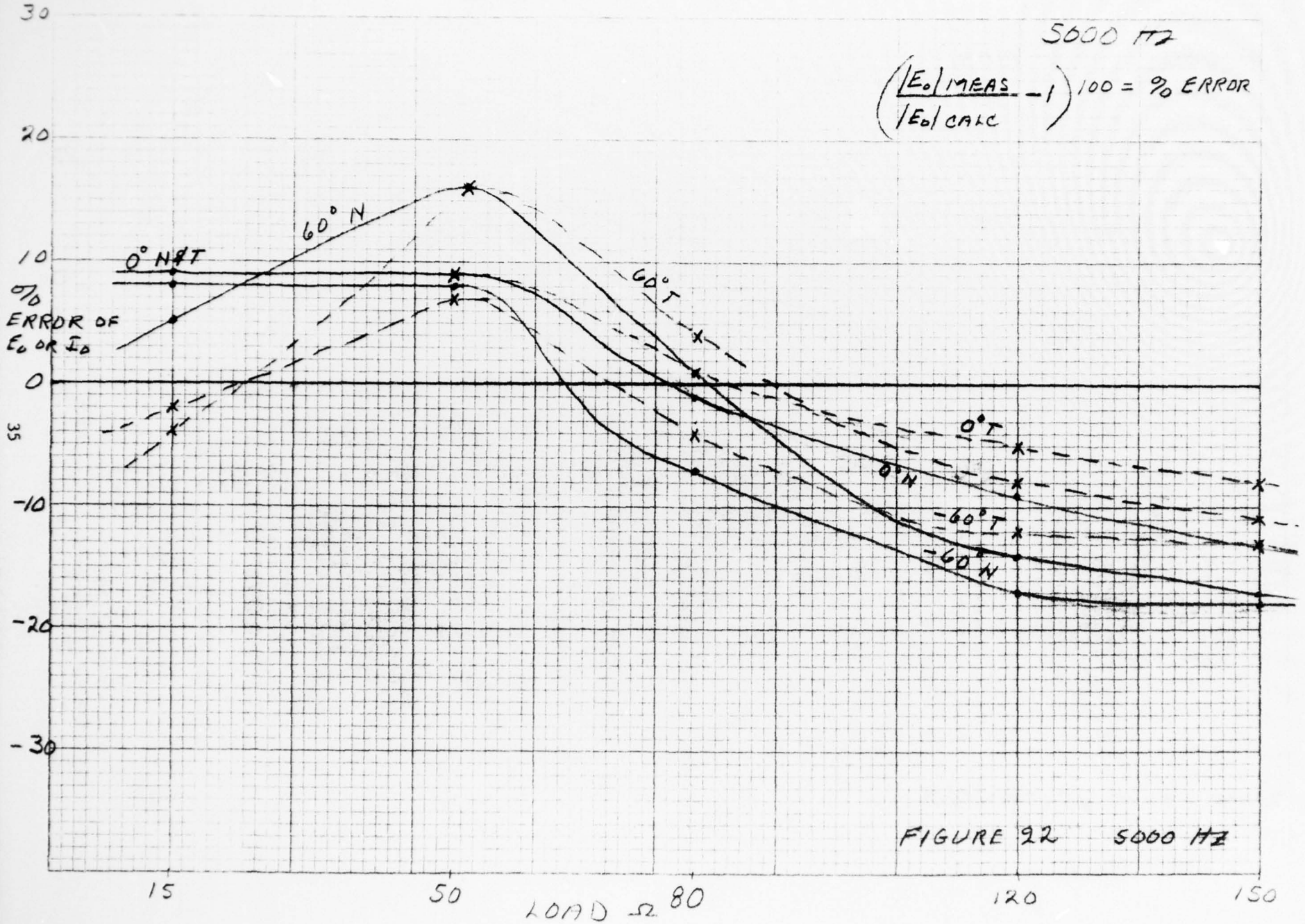

FIGURE 22 5000 HZ

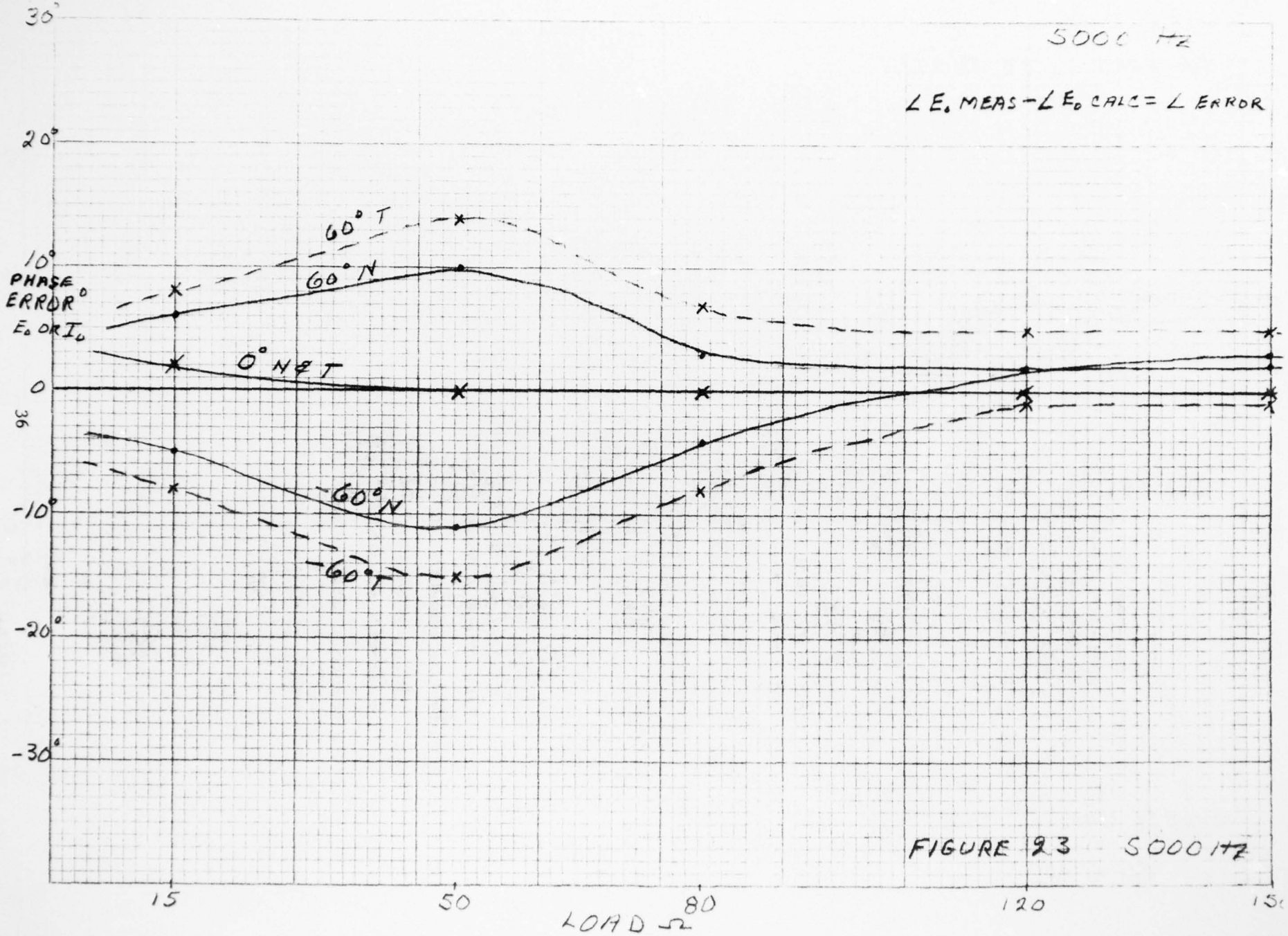

FIGURE 23 5000 Hz

TABLE IX - 5500 Hz

AMPLIFIER LOAD		MAGNITUDE DIFFERENCE IN %				PHASE DIFFERENCE IN DEGREES	
Mag.	Angle	Power Out (NORT)	Power Out (THEV)	E_o & I_o (NORT)	E_o & I_o (THEV)	E_o & I_o (NORT)	E_o & I_o (THEV)
15	- 60°	19	3	9	1	- 3	- 5
	- 30°	20	4	10	2	- 1	- 3
	0°	18	1	9	0	3	3
	30°	19	- 1	9	- 1	6	6
	60°	23	- 2	12	- 1	8	10
50	- 60°	17	13	8	6	- 8	- 11
	- 30°	17	15	8	8	- 4	- 5
	0°	17	14	8	7	- 1	0
	30°	11	9	5	4	2	5
	60°	15	7	7	4	8	15
80	- 60°	15	18	7	9	- 10	- 13
	- 30°	12	15	6	7	- 7	- 8
	0°	- 2	2	- 1	1	- 2	- 2
	30°	- 14	- 8	- 7	- 4	2	4
	60°	- 34	- 26	- 19	- 14	5	9
120	- 60°	- 4	3	- 2	2	- 4	- 7
	- 30°	- 8	- 1	- 4	- 1	- 2	4
	0°	- 15	- 8	- 8	- 4	0	0
	30°	- 26	- 18	- 14	- 9	3	5
	60°	- 40	- 30	- 23	- 16	8	11
150	- 60°						
	- 30°	- 12	- 4	- 6	- 3	0	- 2
	0°	- 22	- 13	- 11	- 7	2	2
	30°	- 31	- 21	- 17	- 11	5	6
	60°	- 44	- 32	- 25	- 18	10	12

Magnitude and phase angle comparisons of measured vs predicted voltage, current and power.

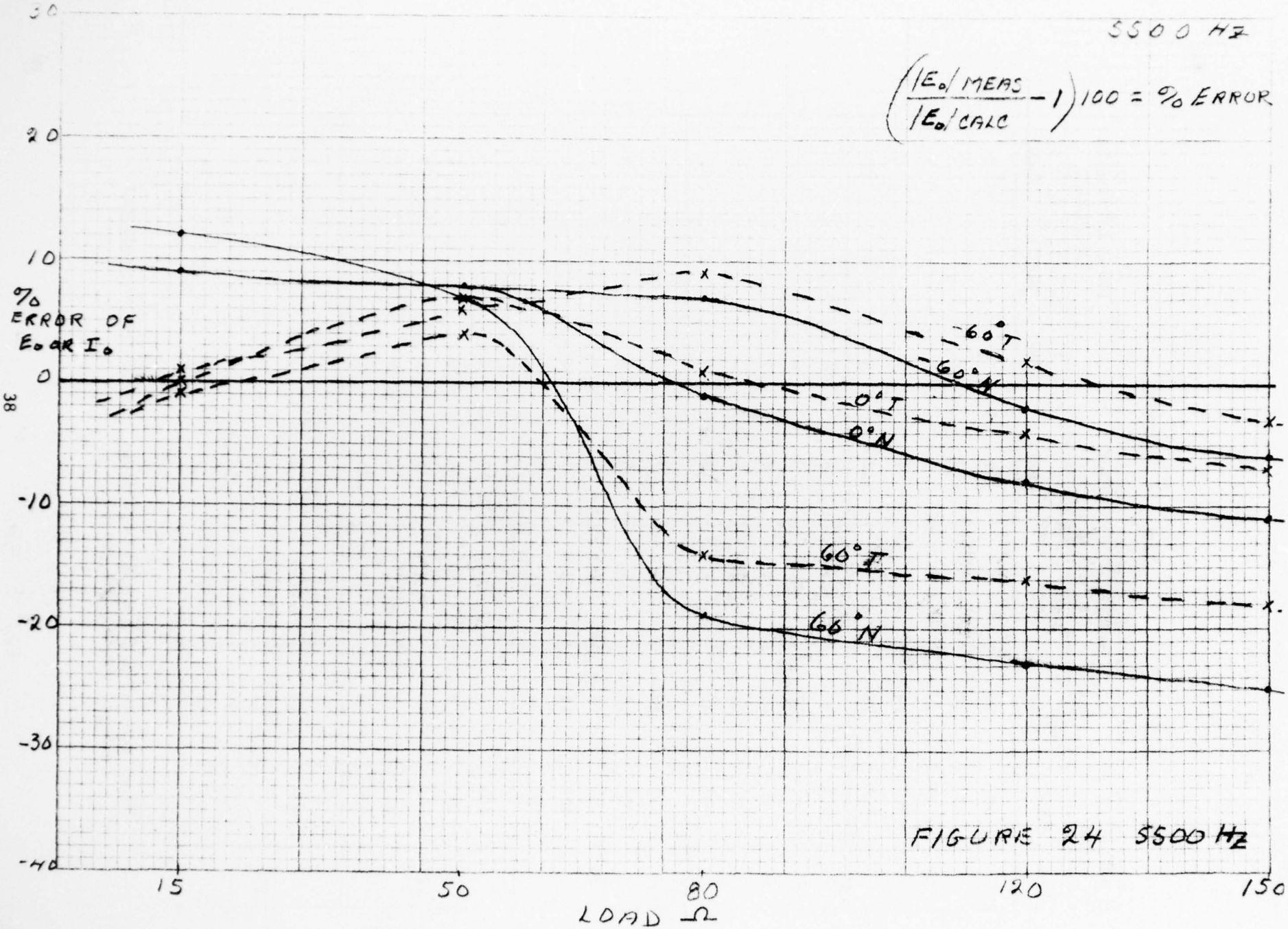

FIGURE 24 5500 Hz

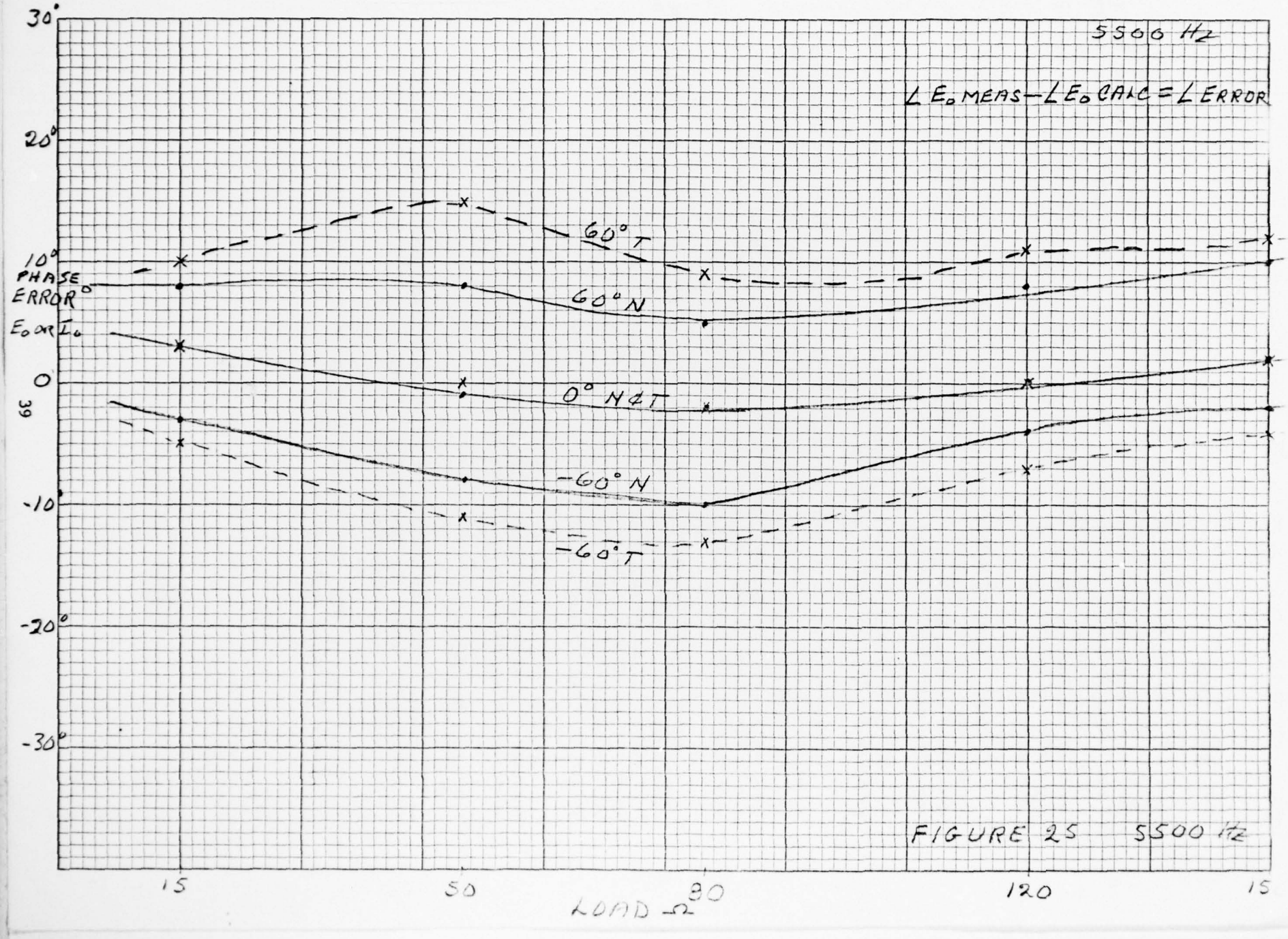

FIGURE 25 5500 Hz

7.0 Ruminations

I think that in a general sense our measurements tend to corrobrate the results published by the manufacturer, however there are certain discrepancies plus some omissions by the manufacturer. The output powers differ somewhat but I think that is mostly in the method of measurement. We measured only the fundamental while he measured total power including harmonics. Input power to the anode of the Neotron tube is the greatest portion of the total input power but still not the whole input power and overall efficiency calculations should take this into account.

We found considerable distortion in the output waveforms, something the manufacturer did not mention. Some of this was due to distortion generated in the driver section but even with a substitute driver which put out a clean signal we still had distorted output waveforms.

We had no problem cooling a single module but no attempt was made to study problems involved in cooling multiple modules.

We made no attempt to test the amplifier for ruggedness either physically or electronically. There is no built-in electronic protection. The amplifier was inadvertently overdriven which caused an arcover from anode to ground but apparently caused no damage. No load less than 15 ohms magnitude was placed across the 50 ohm output tap so we are not sure what would happen if the output were shorted. Probably the fuse in the power supply would go.

I tried to make comparisons between models of this amplifier and some of the other sonar amplifiers which have been modeled. However no criteria or pattern has been set as far as percentage range of load magnitude and phase to be used, so no direct comparison could be made. However as a general feeling the disparity between measured and predicted linear amplifier data for this amplifier is no better in a broad sense and is worse in some specific areas.

Looking over the range of loads used, I think it was a mistake not to have included 30 ohms because there is too great a gap between 15 ohms and 50 ohms. However I do not think it would make much of a change in the overall data.

8.0 Other References

1. B. Green, A. Hirtler and D.A. Steen, Amperex Electronics Corp., "Final Development Report for Feasibility Investigation of A Neotron In A Conduction-Cooled Sonar Amplifier Module".

2. Fred A. Dexter, NUC, "The Evaluation of the Neotron As A Power Amplifying Device for Sonar Applications".

ADDENDUM TO

NURDC TECH NOTE #517 -

"Evaluation of Neotron Sonar Amplifier Module"
by
J. M. Christian

A. We were asked to discuss Part I, Division 2.1, entitled Specifications for Contract Requirements, of the "Final Development Report for Feasibility Investigation of A Neotron In a Conduction-Cooled Sonar Amplifier Module", produced by the Amperex Electronic Corporation.

This discussion is strictly in the light of our evaluation of the Neotron sonar amplifier module and with very meager knowledge of the details of the SQS-23 sonar system. Division 2.1 has nine sections. (a-i)

Section (a) concerns the physical size of the module whose dimensions are 8 1/2" wide, 7" high and 12 7/8" deep. This fits well within the requirements of 12" wide, 7" high and 14" deep. The physical layout and cabling seems to be adequate. We had no trouble with arcover of high voltages except when the amplifier was inadvertently overdriven. This arcover from anode to ground caused no permanent damage. The only real criticism of the physical layout is of the possible frailness of the high voltage plug-in connector on the rear of the module, but this could be ruggedized.

Section (b) calls for the module output power to be variable between 50 and 2500 watts for a 50 ohm non reactive load by varying the anode voltage. Figure (15) of our report shows the power out as a function of DC anode voltage. The power out is controllable in this manner but the already distorted waveforms certainly suffer as the anode voltage is lowered. This is shown in the waveform pictures of Figure (16).

Section (c) calls for the module to operate at 5k Hz with a bandwidth equal to or better than the present SQS-23 bandwidth. We tested only at 4500 Hz, 5000 Hz and 5500 Hz and did not extend beyond this frequency band. The amplifier power outputs for these three frequencies are shown in Figures (2), (3) and (4).

Section (d) calls for a load impedance range of 15 ohms to 150 ohms magnitude for all phase angles between $\pm$ 60°. The nominal center to be 50 ohms non reactive. The curves of Figures (2), (3) and (4) show the power output response for this range of load magnitudes and phase angles. In most instances the power out was greatest with a 50 ohm load for a constant input level, however the plate efficiency seemed to be highest for an 80 ohm load.

Section (e) calls for the module to deliver full output for any input signal level between 100 and 500 millivolts rms. This is accomplished by setting the gain of the amplifier for the level of input signal to be used. The amplifier modules would do this, however, we found that with the gain set for an input level of 500 millivolts rms, the output power vs input level was very non linear. This is graphed in Figure (14). Also under these conditions there was no output when the input level was below 125 millivolts rms.

Sections (f), (g) and (i) require operation at a maximum pulse length of 5 seconds at a 10% duty cycle. We operated full power at this pulse length and duty rate and experienced no difficulty in cooling. The module uses heat conduction to a water cooled heatsink at the rear of the module for cooling. 25°C tap water was used for cooling.

Section (h) states that the following voltages are available: +5400 V DC, +875 V DC, +325 V DC, +150 V DC, -300 V DC and -500 V DC. The currents available at +5400 V DC is 16 A for a duty cycle of 0.9 seconds on and for 11.1 seconds off. The +875 V DC source will deliver 2.9A for the same duty cycle. The +325 V DC source can deliver 3A for 0.9 seconds then 1A for the next 11.1 seconds. With these voltages available, and from our meager knowledge of the SQS-23 system, only the +54-0 V DC source seems capable of supplying the required DC power for the sonar source. This drastically limits the type of amplifier which could be used with these power sources, particularly if space limitation precludes power conversion to a lower voltage - higher current source. This virtually eliminates the use of a high efficiency class D switching type amplifier. This voltage then essentially demands a tube type amplifier. This does not preclude someone more familiar with the entire system from possibly coming up with a solution whereby the system could be changed to provide a different set of voltages from the primary power available. Thus making the use of another type of amplifier possible.

B. In a general criticism of the amplifier module we found that the module seemed to meet the specifications as set forth in the manufacturers version of the contract requirements. Whether the module is an improvement over the present SQS-23 sonar amplifier is a decision that someone more familiar with the SQS-23 system should make. For example the amount of distortion in the output voltage and current waveforms may or may not be tolerable by the system. This distortion is discussed in the evaluation report in terms of both total and individule harmonic levels.

In general the amount of total harmonic distortion in the amplifier output signals has little meaning as far as a specific underwater sound transducer or array system is concerned. Usually only those harmonics which coincide with a frequency where the transducer has a high source per ampere or a high source per volt will produce an unwanted signal at an objectionable level. However each case must be considered separately and someone must make the decision as to the level of unwanted signal that can be tolerated.

C. As an after thought and because it may not be obvious that this is correct, perhaps I should include the calculations upon which we based the decision to use the average value, instead of the true-rms value, of the anode current to calculate the anode input power, as was discussed on page 8a.

The average value of the anode input power

$$P_{avg} = \frac{1}{T} \int_o^T V(t)\ I(t)\ dt$$

where V(t) is a constant and

$$I(t) = b_o + \sum_{n=1}^{\infty} (b_n \text{ Cos } n\omega t + a_n \text{ sin } n\omega t)$$

then

$$P_{avg} = \frac{V}{T} \int_o^T b_o + \sum_{n=1}^{\infty} (b_n \text{ Cos } n\omega t + a_n \text{ sin } n\omega t)\ dt$$

$$= \frac{V}{T} \left[bot + \sum_{n=1}^{\infty} \left(\frac{b_n}{n\omega} \text{ sin } n\omega t - \frac{a_n}{n\omega} \text{ cos } n\omega t \right) \right]_o^T$$

$$= \frac{V}{T} \left\{ b_o T + \sum_{n=1}^{\infty} \left[\frac{b_n T}{2n\pi} \text{ sin } 2n\pi - \frac{a_n T}{2n\pi} \left(\cos 2n\pi - (1)^n \right) \right] \right\}$$

$$= V x b_o + 0$$

$$= V x b_o$$

where b_o is defined as the DC component of the current waveform and

$$\omega = \frac{2\pi}{T}$$